A Novel Finite Element Discretization of Domains with Spheroidal Geometry

Except where reference is made to the work of others, the work described in this dissertation is my own or was done in collaboration with my advisory committee. This dissertation does not include proprietary or classified information.

Necibe Tuncer

Certificate of Approval:

Paul Schmidt
Professor
Mathematics and Statistics

Amnon J. Meir, Chair
Professor
Mathematics and Statistics

Georg Hetzer
Professor
Mathematics and Statistics

Richard Zalik
Professor
Mathematics and Statistics

George T. Flowers
Interim Dean
Graduate School

A Novel Finite Element Discretization of Domains with Spheroidal Geometry

Necibe Tuncer

A Dissertation

Submitted to

the Graduate Faculty of

Auburn University

in Partial Fulfillment of the

Requirements for the

Degree of

Doctor of Philosophy

Auburn, Alabama
May 10, 2007

A Novel Finite Element Discretization of Domains with Spheroidal Geometry

Necibe Tuncer

Signature of Author

Date of Graduation

Dissertation Abstract

A Novel Finite Element Discretization of Domains with Spheroidal Geometry

Necibe Tuncer

Doctor of Philosophy, May 10, 2007
(M.A.,Dokuz Eylul University, 2001)
(B.S., Dokuz Eylul University, 1999)

66 Typed Pages

Directed by Amnon J. Meir

We describe and analyze a new finite element discretizations for domains with spheroidal geometry. In particular, we describe how the method can be used to approximate solutions as well as eigenvalues and eigenfunctions of partial differential equations posed on the sphere, ellipsoidal shell, and cylindrical shell. These novel, so-called, "radially projected finite elements" are particularly attractive for numerical simulations since the resulting finite element discretization is "logically rectangular" and may be easily implemented or incorporated into existing finite element codes.

Style manual or journal used Journal of Approximation Theory (together with the style known as "aums"). Bibliograpy follows van Leunen's *A Handbook for Scholars.*

Computer software used The document preparation package TEX (specifically LATEX) together with the departmental style-file `aums.sty`.

Table of Contents

List of Figures

Chapter 1

Introduction

1.1 Overview

Mathematical models of many engineering and scientific problems usually consist of partial differential equations and some given conditions. The solution of such problems can be approximated by numerical solution techniques. Scientific computing gained significant importance in studies of physical problems. The Finite Element Method (FEM) is a numerical approach to approximate the solution of a partial differential equation. Compared to the Finite Difference Method, the FEM is a fairly new method. FEM has become a favorite method immediately, since it is very easy to use even for complex domains, for general boundary value problems, and also has a strong theoretical basis which yields easy derivation of error estimates. The FEM is very nicely structured so that a general computer program can be used to approximate solutions of various problems easily. Despite all the advantages of the FEM, it is mainly convenient for domains that have a polyhedral geometry. Thus, it has mainly been applied to the polygonal and polyhedral domains. Many studies have been performed for FEM disretization of curved domains or domains with spherical geometry. However, the results of these studies have focused on approximating the domain by a polygonal domain, rather than applying FEM to these exact domains. Recently, there has been growing interest in finite element discretization of partial differential equations defined on the sphere, since these equations have many applications in areas such as climate modeling or weather forecast and various engineering problems.

1.1.1 Background

Mathematical weather models or climate models consist of partial differential equations posed on a domain which is assumed to be a sphere for the obvious reason. Lately, the study of numerically approximating the solution of partial differential equations defined on the sphere has become a favorite subject. However, this is a challenging problem no matter which numerical method is being applied to approximate the solutions of the equations because of the geometry of the sphere. Finite difference methods, spectral methods, finite element methods, finite volume methods are all numerical techniques that have been applied to approximate the solutions of the partial differential equations on the sphere. Grid generation is an important part of approximating solutions of partial differential equations, since the accuracy of numerical solutions depend on the quality of the grid. Various researchers have used different methods for mesh generations on the sphere, such as, constructing the finite element basis directly on spherical triangles by using barycentric coordinate systems [10], approximating, not just the sphere, but any surface with a polyhedral surface, [9] also [6] and [7]. Both of these approaches, described in [10],[9], yield the optimal convergence rate (which is 2 if linear finite elements are used to approximate the solution, the error is measured in the L^2 norm, and the solution is smooth enough). Although all these approaches result in a nice mesh, they suffer from some weaknesses, such as not discretizing the sphere exactly or requiring multiple computations for each refinement step. Our work aims to overcome these difficulties by developing a new method that discretizes the sphere *exactly* and that can also be easily *implemented* and *incorporated* into existing finite element codes.

1.1.2 Our Contribution

Our work is motivated by a desire for exact finite element discretization of the sphere which is yielding a conforming finite element method. We develop and analyze a method which can also be easily implemented and incorporated into an existing code. In our approach, we disceretize the sphere exactly, rather than approximate it, which has not been done before. The method is also very easy to implement if one knows how to implement finite element methods on planar domains. It requires very little computational effort since all computations are done on a logically rectangular domain. Our primary objective is to develop a finite element discretization of a sphere or a ball. Our method can easily be generalized to other domains, such as cylinders, ellipsoids or tori, and can be used for problems posed on domains with spherical, cylindrical, or toroidal holes. In this work we present our approach for the discretization of the sphere, and the same method can be also used for cylinders, ellipsoids and tori. Basically, one can apply this discretization to any domain that has a spherical, cylindrical, ellipsoidal, or toroidal geometry, which we call spheroidal geometry.

We develop and analyze a novel finite element discretization of domains with spheroidal geometry .We present some computational examples related to some of these domains. We first give an introduction to finite element method in section 1.2, introduce smooth manifolds and Laplace Beltrami operator in section 1.3. In chapter 2 we introduce our new method, in chapter 3 we analyze the method, derive error estimates, and in chapter 4 we present numerical results from computer experiments.

1.2 The Finite Element Method

In this section, we introduce the finite element method and illustrate it with the classical Laplace's equation on a bounded, connected, open domain Ω in $\mathbb{R}^n$. Consider the following boundary value problem,

$$-\Delta u = f \text{ in } \Omega \tag{1.1}$$

$$u = 0 \text{ on } \partial\Omega \tag{1.2}$$

which is also known as Poisson's equation. In (1.1), Δ is the Laplacian, $\partial\Omega$ is the boundary of the domain Ω, and u is the unknown function. The right hand side f is a real valued function defined on the open subset Ω of $\mathbb{R}^n$, we say that $f \in \mathbb{C}^r(\Omega)$, if all the k^{th} order (classical) partial derivatives exist and are continuous for $k \leq r$, where r, k are positive integers. We call any function $u \in \mathbb{C}^2(\Omega)$ that satisfies the differential equation and the boundary condition a classical solution.

Consider the Lebesgue measure of $\mathbb{R}^n$, let Ω be a Lebesgue measurable domain, and let f be a Lebesgue-integrable function, then we denote the Lebesgue integral by

$$\int_\Omega f d\Omega$$

where $d\Omega$ denotes the Lebesgue measure. We say that f is in $L^p(\Omega)$, for $1 \leq p < \infty$ if $\left(\int_\Omega |f|^p d\Omega\right)^{1/p} < \infty$. The set, $L^p(\Omega)$ is a Banach space, with the following norm,

$$\|f\|_{L^p(\Omega)} := \left(\int_\Omega |f|^p d\Omega\right)^{1/p}.$$

The Sobolev spaces $W^{m,p}(\Omega)$ are defined to be the set of all functions $f \in L^p(\Omega)$ that have weak derivatives in $L^p(\Omega)$ up to order m.

$$W^{m,p}(\Omega) := \{f \in L^p(\Omega) : D^\alpha f \in L^p(\Omega) \quad |\alpha| \leq m\},$$

where D^α is a multi index notation for partial derivatives (in the weak sense), $\alpha = (\alpha_1, \alpha_2, \ldots, \alpha_n)$ is an n-tuple of non-negative integers, and the length of α is denoted by $|\alpha| = \alpha_1 + \alpha_2 + \cdots + \alpha_n$. The Sobolev space $W^{m,p}(\Omega)$ equipped with the norm

$$\|f\|_{W^{m,p}(\Omega)} := \left(\sum_{|\alpha| \leq m} \|D^\alpha f\|^p_{L^p(\Omega)} \right)^{1/p},$$

is a Banach Space. We denote by $W_0^{m,p}(\Omega)$ the closure of $\mathbb{C}_c^m(\Omega)$ in $W^{m,p}(\Omega)$. We denote by $\mathbb{C}_c^m(\Omega)$ the space of functions $u \in \mathbb{C}^m(\Omega)$ that have compact support. Also, we denote by $H^m(\Omega)$, the spaces $H^m(\Omega) = W^{m,2}(\Omega)$, these are the Hilbert spaces. Note that $H_0^1(\Omega)$ is the subspace of $H^1(\Omega)$ and consists of the functions that are zero on $\partial\Omega$ in the sense of traces.

A variational formulation of problem (1.1), can be derived by multiplying the both sides of (1.1) by functions v in $H_0^1(\Omega)$. Then by integration by parts we get,

$$\int_\Omega \nabla u \cdot \nabla v d\Omega = \int_\Omega f \cdot v d\Omega.$$

Now the solution u is required to only be in $H_0^1(\Omega)$, which means we look for a solution in a bigger set. In this case we say that u is a weak solution of (1.1). The new problem:

$$\text{Find } u \in H_0^1(\Omega) \text{ such that } \int_\Omega \nabla u \cdot \nabla v d\Omega = \int_\Omega f \cdot v d\Omega \quad \forall v \in H_0^1(\Omega) \tag{1.3}$$

This is called a weak or variational formulation of (1.1). We define the bilinear form $a(u,v) : H_0^1(\Omega) \times H_0^1(\Omega) \to \mathbb{R}$ as $a(u,v) := \int_\Omega \nabla u \cdot \nabla v d\Omega$, which is also known as the energy inner product. Similarly, $(f,v) := \int_\Omega f \cdot v d\Omega$, is the standard inner product in $L^2(\Omega)$. We say that a bilinear form $a(u,v) : H_0^1(\Omega) \times H_0^1(\Omega) \to \mathbb{R}$ is *elliptic* if there exists $\alpha > 0$ such that

$$a(v,v) \geq \alpha \|v\|^2_{H^1(\Omega)} \; \forall v \in H_0^1(\Omega).$$

We say that the the bilinear form is *continuous* or *bounded* if there exists a constant $C > 0$ such that

$$a(u,v) \leq C \|u\|_{H_0^1(\Omega)} \|v\|_{H_0^1(\Omega)}.$$

Clearly, $a(\cdot,\cdot)$ induces a norm, which is equivalent to the norm of the Hilbert space $H_0^1(\Omega)$. This norm

$$\|v\|_a = \sqrt{a(v,v)}$$

is called the energy norm. The question we need to answer is the relationship between (1.1) and its variational problem (1.3). Let $f \in L^2(\Omega)$ and $u \in H^2(\Omega)$ then u satisfies (1.3) if and only if u is a solution of (1.1).

Within the theory of functional analysis, one can prove the following theorem, which is known as Riesz Representation theorem in the literature [12].

Theorem 1.1 *Let H be a Hilbert space and let L be a continuous linear functional $L : H \to \mathbb{R}$, s.t. $L(u) = (u, v)\ \forall u \in H$ then L is an isomorphism.*

Theorem 1.2 *There exists a unique solution to (1.3).*

Proof: The bilinear form $a(\cdot, \cdot)$ is a bounded, elliptic such that $(H_0^1(\Omega), a(\cdot, \cdot))$is a Hilbert space. Then the theorem follows as a consequence of Riesz representation theorem. □

To approximate the solution of (1.3), we construct the discrete variational problem in a finite dimensional subspace of $H_0^1(\Omega)$. Let χ be the finite dimensional subspace of $H_0^1(\Omega)$, then the discrete analog of problem (1.3) is :

$$\text{Find } u_h \in \chi \text{ such that } \int_\Omega \nabla u_h \cdot \nabla v_h d\Omega = \int_\Omega f \cdot v_h d\Omega \quad \forall v_h \in \chi. \tag{1.4}$$

It is worth noting that by (1.4), we construct a discrete scheme for approximating the solution of (1.1). Also, at this point we need to remark that (1.4) has a unique solution, since χ together with the bilinear form, $a_h(u_h, v_h) := \int_\Omega \nabla u_h \cdot \nabla v_h d\Omega$ is a Hilbert space.

1.2.1 Discretization of the Domain and Basis Elements

Finite element method can be used to solve the discrete problem (1.4). One important step is to define, χ, the finite dimensional subspace of $H_0^1(\Omega)$. We define χ by first partitioning the domain. For simplicity, hereinafter let Ω be a convex polygonal domain in $\mathbb{R}^2$. Let $\mathcal{K}_1, \mathcal{K}_2, \ldots, \mathcal{K}_n$ be triangles or quadrilaterals such that they form a partition of Ω, i.e

$$\Omega = \bigcup_{i=1}^{n} \mathcal{K}_i \text{ and } \mathring{\mathcal{K}}_i \bigcap \mathring{\mathcal{K}}_j = \emptyset.$$

For any intersection of two triangles or quadrilaterals $\mathcal{K}_i$ and $\mathcal{K}_j$, if the intersection consists of one point then it is a common vertex, if the intersection consists of more than one point then it is a common edge. Let $\mathcal{T}^j = \{\mathcal{K}_1^j, \mathcal{K}_2^j, \ldots, \mathcal{K}_{n_j}^j\}$, $j \in \mathbb{N}$ denote the family of triangulation where j denotes the refinement step. We say that the mesh size of the triangulation $\mathcal{T}$ at the j^{th} refinement step is h^j where

$$h^j = \max_{\mathcal{K}_i^j \in \mathcal{T}^j} h_{\mathcal{K}_i^j}, \quad \text{and} \quad h_{\mathcal{K}_i^j} = \operatorname{diam}(\mathcal{K}_i^j),$$

here $\operatorname{diam}(\mathcal{K}_i^j) = \sup_{x,y \in \mathcal{K}_i^j} \|x - y\|$.

The quantity h^j is a measure of how refined the mesh is. The smaller h^j is, the finer the mesh. Let $\rho_{\mathcal{K}_i^j}$ denote the radius of inscribed circle in $\mathcal{K}_i^j$. We say that a family of triangulation $\mathcal{T}^j$, $j \in \mathbb{N}$ is *shape regular* if there exists a constant $\kappa > 0$, independent of j such that for each $\mathcal{K}_i^j \in \mathcal{T}^j$, we have

$$\frac{h_{\mathcal{K}_i^j}}{\rho_{\mathcal{K}_i^j}} \leq \kappa.$$

Figure 1.1 shows a uniform triangulation of the square. Usually we choose the finite dimensional subspace to be the space of piecewise polynomials on the domain Ω. Piecewise linear or quadratic functions are widely used in defining these subspaces. Figure 1.2 shows the linear basis element. For instance, define χ to be the space of piecewise linear polynomials, that is:

$$\chi = \{\omega : \omega \text{ is piecewise linear continuous polynomials and } \omega = 0 \text{ on } \partial\Omega\}.$$

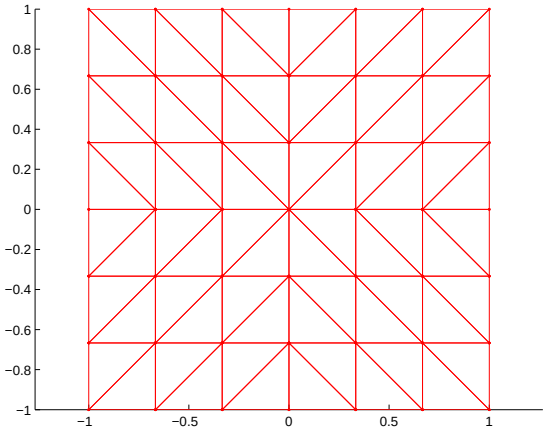

Figure 1.1: A uniform triangulation of the square

Let $\{\omega_i\}_i^n$ be a basis for χ, then for any $u_h \in \chi$ we have $u_h = \sum_i^n u_i\omega_i$. Thus, (1.4) reduces to a linear system of equations of the following form

$$Au = f$$

where A is a $n \times n$ matrix whose entries are $A_{ij} = a_h(\omega_j, \omega_i)$, and $\mathbf{u}$ and $\mathbf{f}$ are $n \times 1$ vectors of the form $\mathbf{u}(i) = u_i$, $\mathbf{f}(i) = (f, \omega_i)$. Since the bilinear form $a_h(\cdot, \cdot)$ is symmetric and elliptic, the matrix A is symmetric and positive definite, which assures the existence and uniqueness of a solution of (1.4). The matrix A is also a sparse matrix, if the basis functions are chosen to have compact support. In the following section we talk about the error estimates in the finite element method.

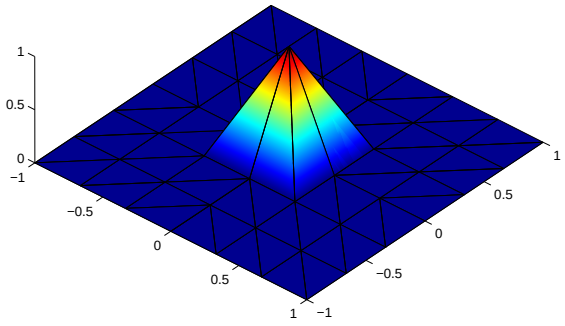

Figure 1.2: Linear basis element

1.2.2 Error Estimates

Let u_h be the solution of (1.4) and u be the exact solution of (1.3), we first observe the orthogonality between $u - u_h$ and u_h in terms of the energy inner product. Simply, subtracting, (1.4) from (1.3), we get,

$$a(u - u_h, v_h) = 0, \forall v_h \in \chi. \tag{1.5}$$

The following lemma, which is known as Cea's lemma, plays a significant role in establishing error estimates in finite element method.

Lemma 1.1 *(Cea's Lemma) Let u_h be the solution of (1.4) and u be the exact solution of (1.3), then*

$$\|u - u_h\|_{H^1(\Omega)} \leq \frac{C}{\alpha} \inf_{v_h \in \chi} \|u - v_h\|_{H^1(\Omega)}.$$

Proof: The bilinear form is elliptic, $a(u-u_h, u-u_h) \geq \alpha \|u-u_h\|^2_{H^1(\Omega)}$ and $a(u-u_h, u-u_h) = a(u-u_h, u-v_h)$, since $a(u-u_h, u_h-v_h) = 0$ from (1.5) and the bilinear form is continuous, that is,

$$\begin{aligned} a(u-u_h, u-v_h) &\leq C\|u-u_h\|_{H^1(\Omega)}\|u-v_h\|_{H^1(\Omega)} \\ \alpha\|u-u_h\|^2_{H^1(\Omega)} &\leq C\|u-u_h\|_{H^1(\Omega)}\|u-v_h\|_{H^1(\Omega)} \\ \|u-u_h\|_{H^1(\Omega)} &\leq \frac{C}{\alpha}\|u-v_h\|_{H^1(\Omega)}. \end{aligned}$$

□

Cea's Lemma states that the solution of (1.4) is a best approximation to the solution of (1.3) by an element of χ. Since, Ω is a convex polygonal domain in $\mathbb{R}^2$, by Sobolev Embedding theorem, $H^2(\Omega)$ is continuously imbedded in $C(\bar{\Omega})$. Thus, for every $u \in H^2(\Omega)$, there exists a uniquely defined interpolation operator, $\mathcal{I}u$, associated with the nodal points. In the theory of finite elements one can prove the following theorem which states the convergence rates of the finite element method [11].

Theorem 1.3 *Let $u \in H^2(\Omega)$ and $\mathcal{T}$ be a shape regular triangulation of Ω, and $\mathcal{I}$ be an interpolation operator $\mathcal{I} : H^2(\Omega) \to P_{t-1}$, where P_{t-1} denotes the space of piecewise polynomial functions of degree $\leq t-1$, then there exists a constant c such that*

$$\|u - \mathcal{I}u\|_{H^m(\mathcal{K}_i)} \leq ch^{t-m}|u|_{H^t(\mathcal{K}_i)} \quad \text{for } u \in H^2(\Omega), \quad 0 \leq m \leq t,\ t = 2.$$

1.3 Smooth Manifolds

We are interested in finite element discretization of spheres, ellipsoids, cylinders and tori or geometries that we generally call spheroidal geometries. Spheres are smooth manifolds in $\mathbb{R}^3$, or genereally in $\mathbb{R}^n$. In this section, we give a brief introduction to manifolds and define the Laplace-Beltrami operator on smooth manifolds. Before introducing smooth manifolds, let's first define topological manifolds.

Definition 1.1 *A set X together with the collection of its subsets, J, form a topology if*

- $X, \emptyset \in J$,
- *union of any sets that are in J is also in J*
- *the intersection of any two sets that are in J is also in J.*

We call these sets that are in J the open sets.

A special case of topological spaces is a Hausdorff space. It is a topological space with the property that for every two distinct points x, y in X, there exists an open neighborhood U of x and an open neighborhood V of y, which are distinct as well. The definition of k-dimensional topological manifold, $M \neq \emptyset,\ M \subset \mathbb{R}^n$, is given in [1] as a Haussdorff, second countable topological space that is locally homeomorphic (one-to-one, onto, continuous and has a continuous inverse) to $\mathbb{R}^k$. In other words, topological manifolds are the spaces that locally look like Euclidean spaces.

Example The unit sphere, $\mathcal{S}^2$, in $\mathbb{R}^3$ is a 2-dimensional topological manifold.

The unit sphere, $\mathcal{S}^2$, is the set of unit vectors in $\mathbb{R}^3$, that is

$$\mathcal{S}^2 = \{x = (x_1, x_2, x_3),\ x \in \mathbb{R}^3 : |x| = 1\}.$$

The unit sphere, $\mathcal{S}^2$, is by definition a topological subspace of $\mathbb{R}^3$. Thus, it is Haussdorff and second countable. We need to show that it is locally Euclidean. To show that it is locally homeomorphic to $\mathbb{R}^2$, we need to show that for every point p in $\mathcal{S}^2$, there exists a homeomorphism, $\varphi : U \subset \mathcal{S}^2 \to V \subset \mathbb{R}^2$ between the open neighborhood U of p and a open subset V of $\mathbb{R}^2$. Let U_i^+ denote the subset of $\mathcal{S}^2$ such that i^{th} coordinate is positive, for $i = 1, 2, 3$. Similarly, let U_i^- denote the subset of $\mathcal{S}^2$ such that i^{th} coordinate is negative, for $i = 1, 2, 3$,

$$\begin{aligned} U_i^+ &= \{(x_1, x_2, x_3) \in \mathcal{S}^2 : x_i > 0\}\ i = 1, 2, 3, \\ U_i^- &= \{(x_1, x_2, x_3) \in \mathcal{S}^2 : x_i < 0\}\ i = 1, 2, 3. \end{aligned}$$

Let $\varphi_{U_i^+} : U_i^+ \to \mathbb{R}^2$ denote the homeomorphisms from U_i^+ to $\varphi_{U_i^+}(U_i^+) \subset \mathbb{R}^2$, for $i = 1, 2, 3$, which are defined as

$$\begin{aligned}
&\varphi_{U_1^+}(x_1, x_2, x_3) = (x_2, x_3), && \varphi^{-1}_{U_1^+}(x_2, x_3) = (\sqrt{1 - (x_2^2 + x_3^2)}, x_2, x_3), \\
&\varphi_{U_2^+}(x_1, x_2, x_3) = (x_1, x_3), && \varphi^{-1}_{U_2^+}(x_1, x_3) = (x_1, \sqrt{1 - (x_1^2 + x_3^2)}, x_3), \\
&\varphi_{U_3^+}(x_1, x_2, x_3) = (x_1, x_2), && \varphi^{-1}_{U_3^+}(x_1, x_2) = (x_1, x_2, \sqrt{1 - (x_1^2 + x_2^2)}), \\
&\varphi_{U_1^-}(x_1, x_2, x_3) = (x_2, x_3), && \varphi^{-1}_{U_1^-}(x_2, x_3) = (-\sqrt{1 - (x_2^2 + x_3^2)}, x_2, x_3), \\
&\varphi_{U_2^-}(x_1, x_2, x_3) = (x_1, x_3), && \varphi^{-1}_{U_2^-}(x_1, x_3) = (x_1, -\sqrt{1 - (x_1^2 + x_3^2)}, x_3), \\
&\varphi_{U_3^-}(x_1, x_2, x_3) = (x_1, x_2), && \varphi^{-1}_{U_3^-}(x_1, x_2) = (x_1, x_2, -\sqrt{1 - (x_1^2 + x_2^2)}).
\end{aligned}$$

Thus, the unit sphere in $\mathbb{R}^3$ is 2-dimensional topological manifold.

Let U be an open subset of M and let $\varphi : U \to \varphi(U) \subset \mathbb{R}^k$ be a homeomorphism then we call the pair (U, φ) a chart. If p is a point in U we say that the pair (U, φ) is a chart at p, and we call U the coordinate neighborhood of p, and we call the Cartesian coordinates of p, $\varphi(p) = (\varphi_1(p), \varphi_2(p), \ldots, \varphi_k(p)) = (x_1, x_2, \ldots, x_k) \in \mathbb{R}^k$ the coordinates of p.

Definition 1.2 *A function $f : M \to \mathbb{R}$ is continuous at $p \in M$, if for some chart (U, φ) at p, $f \circ \varphi^{-1} : \varphi(U) \to \mathbb{R}$ is continuous at $\varphi(p)$. The function $f : M \to \mathbb{R}$ is continuous on the open set $U \subset M$, if it is continuous at all points p in U.*

If M is a topological manifold, the notion of a continuous function $f : M \to \mathbb{R}$ makes sense, but the notion of a differentiable function does not, since differentiablity property of a function is not invariant under homeomorphism. We need to add more features to a topological manifold and get a smooth manifold. We say that f is smooth, if $f \in \mathbb{C}^\infty(U)$, that is if $f \in \mathbb{C}^r(U)$ for every r. The function f is said to be a diffeomorphism, if f and its inverse f^{-1} are smooth.

Definition 1.3 *Let (U, φ) and (V, ψ) be two charts, such that $U \bigcap V \neq \emptyset$, the charts (U, φ) and (V, ψ) are called $\mathbb{C}^\infty$-compatible if the transition map $\psi \circ \varphi^{-1} : \varphi(U \bigcap V) \to \psi(U \bigcap V)$ is a diffeomorphism.*

If we index the charts, $(U_i, \varphi_i),\ i \in I$ where i ranges over some index set I, such that the sets U_i cover M, then we call such a collection of charts an *atlas* and denote it by $\mathcal{A}$. An atlas $\mathcal{A}$ is called a *differential structure* if (U, φ) is a chart in M such that it is compatible with every chart in M, then (U, φ) is in $\mathcal{A}$.

Definition 1.4 *The pair $(M, \mathcal{A})$ is a smooth manifold, where M is a topological manifold and $\mathcal{A}$ is a differential structure [2].*

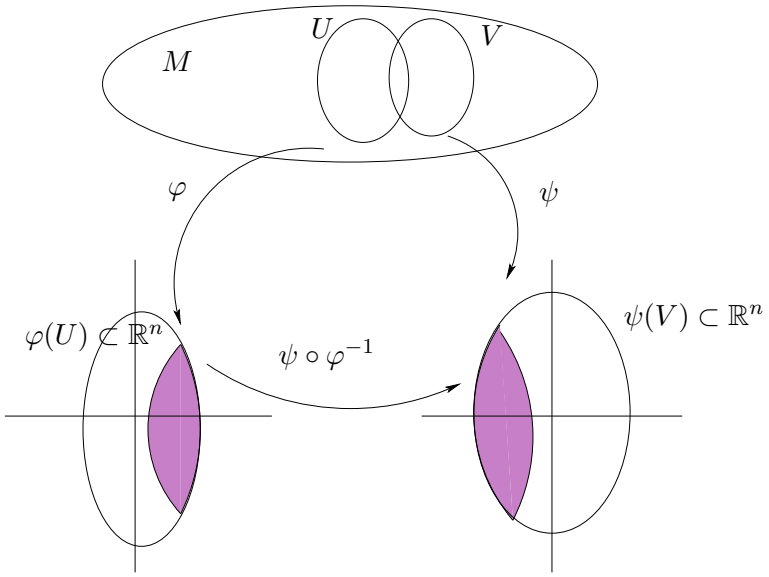

Figure 1.3: A transition map

We usually omit the differential structure and say *M is a smooth manifold*. A smooth manifold is a topological manifold whose transitions maps are all smooth. For more detailed information on smooth manifolds see [2].

Example The unit sphere, $\mathcal{S}^2$, in $\mathbb{R}^3$ is a 2-dimensional smooth manifold. Since, it is clear from the previous example that $\{U_i^+, U_i^-, i = 1, 2, 3\}$ is an open cover for $\mathcal{S}^2$. For simplicity, let's consider, $U_1^+ \bigcap U_1^- = \{(x_1, x_2, x_3) \in \mathcal{S}^2 : x_1 > 0, x_2 > 0\}$, then the transition maps, $\varphi_{U_1^+} \circ \varphi_{U_2^+}^{-1} = (\sqrt{1 - (x_1^2 + x_2^2)}, x_3)$ and $\varphi_{U_2^+} \circ \varphi_{U_1^+}^{-1} = (\sqrt{1 - (x_2^2 + x_3^2)}, x_3)$ are compatible. Any other pair can be shown to be compatible, in a similar way. Furthermore, the unit sphere is a compact smooth manifold.

Definition 1.5 *A function $f : M \to \mathbb{R}$ is smooth ($\mathbb{C}^\infty(M)$) if and only if f is continuous and for every p in M, and there exists a chart (U, φ) at p such that $f \circ \varphi^{-1} : \varphi(U) \to \mathbb{R}$ is smooth ($\mathbb{C}^\infty((\varphi(U))$.*

This definition is well defined, since it is independent of the choice of the the chart at p. We can generalize this definition easily to smooth maps between smooth manifolds. Let $M \neq \emptyset,\ M \subset \mathbb{R}^n$, be k-dimensional smooth manifold and $N \neq \emptyset,\ N \subset \mathbb{R}^n$ be l-dimensional smooth manifold, the mapping $F : M \to N$ is a smooth mapping, if and only if F is continuous and for every $p \in M$, there exists a chart (U, φ) in M and a chart (V, ψ) in N such that $F(U) \subset V$, and the mapping $\psi \circ F \circ \varphi^{-1} : \varphi(U) \to \psi(V)$ is smooth.

Tangent Spaces

Hereinafter M denotes k-dimensional smooth submanifold of $\mathbb{R}^n$. We first, define the partial derivatives of a differentiable function $f : M \to \mathbb{R}$ with respect to the coordinate system (U, φ). At this point, it is worth recalling the limit definition of partial derivatives of the function $f : \mathbb{R}^k \to \mathbb{R}$. Let $x = (x_1, \ldots, x_k) \in \mathbb{R}^k$, then we denote by $D_i f(x_1, \ldots .x_k)$, the number

$$\lim_{h \to 0} \frac{f(x_1, \ldots, x_i + h, \ldots, x_k) - f(x_1, \ldots .x_k)}{h}.$$

For a function $f : M \to \mathbb{R}$ and local charts (U, φ), we define

$$D_i f(p) = D_i \left(f \circ \varphi^{-1} \right)(\varphi(p)) . \tag{1.6}$$

Thus, $D_i f(p)$ is the number

$$\lim_{h \to 0} \frac{f\left(\varphi_1^{-1}(x), \ldots, \varphi_i^{-1}(x) + h, \ldots, \varphi_k^{-1}(x)\right) - f(\varphi^{-1}(x))}{h}.$$

If we define the curve $\gamma_i : (-\epsilon, \epsilon) \to M$ by $\gamma_i(h) = (\varphi_1^{-1}(x), \ldots, \varphi_i^{-1}(x) + h, \ldots, \varphi_k^{-1}(x))$, then (1.6) is just

$$(f \circ \gamma_i)'(0) = \lim_{h \to 0} \frac{f(\gamma_i(h)) - f(\gamma_i(0))}{h}.$$

Define the collection of all such $\mathbb{C}^1$ curves in M by

$$\mathcal{C}_p = \{\gamma \in \mathbb{C}^1((\epsilon, \epsilon), M), \epsilon > 0, \gamma(0) = p\}.$$

We say that $x \in \mathbb{R}^n$ is tangent to M at the point p, if and only if there exists a $\gamma \in \mathcal{C}_p$ such that $x = \gamma'(0)$.

Definition 1.6 *We define the tangent space at p as $T_pM = \{(\gamma'(0)) : \gamma \in \mathcal{C}_p\}$, and tangent bundle TM as $TM := \bigcup_{p \in M} T_pM$. An element of TM is an ordered pair (p, x) with $p \in M$ $x \in T_pM$. The* projection map *$\pi : TM \to M$ maps each vector in T_pM to the point at which it is tangent as $\pi(p, x) = p$.*

Remark 1.1 *For any $p \in M$, T_pM is a k-dimensional vector space, and if (U, φ) is chart containing p, then $(D_1\varphi^{-1}, D_2\varphi^{-1}, \ldots, D_k\varphi^{-1})$ forms a basis for T_pM.*

Remark 1.2 *Tangent bundle TM is a $2k$-dimensional manifold and the $\pi : TM \to M$ is a smooth map.*

Definition 1.7 *The tangent map $TF : TM \to TN$ for a $\mathbb{C}^1$-map $F : M \to N$ is defined by*

$$TF(\gamma(0), \gamma'(0)) = (\gamma(0), (F \circ \gamma)'(0)).$$

The differential of F, is a linear mapping $DF : T_pM \to T_{F(p)}N$ which is defined as:

$$F(\gamma'(0)) = (F \circ \gamma)'(0).$$

Define $g_p(\cdot,\cdot) : T_pM \times T_pM \to \mathbb{R}$ as $g_p(x,y) = x \cdot y$, where $x \in T_pM$ $y \in T_pM$ and $x \cdot y$ is the inner product T_pM inherited from $\mathbb{R}^n$. Recall that $(D - 1\varphi^{-1}, D_2\varphi^{-1}, \dots D_k\varphi^{-1})$ is a basis for T_pM, and define the metric tensor $G = g_{ij}$ as

$$g_{ij} = D_i\varphi^{-1} \cdot D_j\varphi^{-1}$$

and $g = \det(G)$ is called the Gramm determinant and is strictly positive. Let $f : M \to \mathbb{R}$ be a differentiable function, then the differential of f is a linear mapping T_pM to $\mathbb{R}$, thus it is a functional on T_pM. So, by the Riesz Representation (Theorem 1.1), there exists a unique vector in T_pM, call it gradient of f, and denote it by ∇f, such that $Df(p)v = \nabla f \cdot v$ for every $v \in T_pM$.

Remark 1.3 *Let $f : M \to \mathbb{R}$ and (U, φ) a chart containg p, then $\nabla f(p)$ is defined as*

$$\nabla f(p) = \sum_{i=1}^{k} \sum_{j=1}^{k} g^{ij} D_j(f \circ \varphi^{-1})(\varphi(p)). \tag{1.7}$$

Definition 1.8 *A vector field is a continuous map $X : M \to TM$, such that $\pi \circ X = Id_M$, that is*

$$X(p) = (p, x(p)) \quad \forall p \in M$$

such that $x(p)$ is a tangent vector to p.

Let X be $\mathbb{C}^1$-vector field on M with local representation $X \circ \varphi = \sum_{i=1}^{k} X^i \partial_i \varphi$, define a scalar function $\nabla \cdot X : M \to \mathbb{R}$ as

$$(\nabla \cdot X) \circ \varphi = \frac{1}{\sqrt{g}} \sum_{i=1}^{k} \partial_i \left(X^i \right).$$

For any $\mathbb{C}^2$ function $f : M \to \mathbb{R}$ define Laplace-Beltrami operator as

$$\Delta f = \nabla \cdot \nabla f.$$

Let φ be a local chart then the local representation is

$$(\Delta f) \circ \varphi = (\nabla \cdot \nabla f) \circ \varphi = \frac{1}{\sqrt{|g|}} \sum_{j=1}^{k} \partial_j (\sqrt{|g|} \sum_{i=1}^{k} g^{ij} \partial_i (f \circ \varphi)) \tag{1.8}$$

where g^{ij} are the components of g^{-1}.

The Laplace Beltrami Operator on the Sphere

Let $\varphi(\theta_1, \theta_2) = (\sin\theta_1 \cos\theta_2, \sin\theta_1 \sin\theta_2, \cos\theta_1) \quad 0 \leq \theta_1 \leq \pi,\ 0 \leq \theta_2 < 2\pi$ be a local chart of the sphere, then

$$g = \begin{pmatrix} \partial_{\theta_1}\varphi \cdot \partial_{\theta_1}\varphi & \partial_{\theta_1}\varphi \cdot \partial_{\theta_2}\varphi \\ \partial_{\theta_2}\varphi \cdot \partial_{\theta_1}\varphi & \partial_{\theta_2}\varphi \cdot \partial_{\theta_2}\varphi \end{pmatrix} = \begin{pmatrix} 1 & 0 \\ 0 & \sin^2\theta_1 \end{pmatrix}$$

and also,

$$g^{-1} = \begin{pmatrix} 1 & 0 \\ 0 & \frac{1}{\sin^2\theta_1} \end{pmatrix} \quad \text{and} \quad |g| = \sin^2\theta_1.$$

We obtain the local representation of the Laplace-Beltrami $\Delta_{\mathcal{S}} f$ of any $\mathbb{C}^2$ function f on the sphere as

$$\begin{aligned}(\Delta_{\mathcal{S}} f)\circ\varphi &= \frac{1}{\sqrt{|g|}}\sum_{j=1}^{2}\partial_j(\sqrt{|g|}\sum_{i=1}^{2} g^{ij}\partial_i(f\circ\varphi)) \\ &= \frac{1}{\sin\theta_1}[\partial_{\theta_1}(\sin\theta_1\partial_{\theta_1}) + \partial_{\theta_2}(\frac{1}{\sin\theta_1}\partial_{\theta_2})](f\circ\varphi) \\ &= \frac{1}{\sin\theta_1}\partial_{\theta_1}(\sin\theta_1\partial_{\theta_1}) + \frac{1}{\sin^2\theta_1}\partial_{\theta_2}(\partial_{\theta_2})f\circ\varphi.\end{aligned} \tag{1.9}$$

1.4 Eigenvalue Problem

Let $\Delta_{\mathcal{S}}$ be the Laplace operator on the sphere, then the eigenvalue problem is to find a scalar λ such that $-\Delta_{\mathcal{S}}\mu = \lambda\mu$. If the local representation of Laplace-Beltrami operator is obtained using polar coordinate charts (1.9), then the eigenvalue problem is given by

$$\frac{1}{\sin\theta_1}\partial\theta_1(\sin\theta_1\partial_{\theta_1}\mu) + \frac{1}{\sin^2\theta_1}\partial_{\theta_2}(\partial_{\theta_2}\mu) = -\lambda\mu. \tag{1.10}$$

Writing μ in separable form $\mu(\theta_1,\theta_2) = \nu(\theta_1)\rho(\theta_2)$, we obtain the following two eigenvalue problems

$$\frac{d^2\rho}{d\theta_2^2} + \zeta\rho = 0 \quad \rho(0) = \rho(2\pi),\ \frac{d\rho}{d\theta_2}(0) = \frac{d\rho}{d\theta_2}(2\pi) \tag{1.11}$$

and

$$\sin\theta_1\frac{d}{d\theta_1}(\sin\theta_1\frac{d\nu}{d\theta_1}) + (\lambda\sin^2\theta_1 - \zeta)\nu = 0, \quad \lim_{\theta_1\to 0}\nu < \infty,\ \lim_{\theta_1\to\pi}\nu < \infty. \tag{1.12}$$

Eigenvalues and the corresponding eigenfunctions of the problem (1.11) are

$$\zeta_m = m^2, \quad \rho(\theta_2) = A_m \cos m\theta_2 + B_m \sin m\theta_2, \ m = 0, 1, 2 \ldots .$$

Substituting the eigenvalues ζ_m and $t = \cos\theta_1$ into (1.12), and setting $P(t) = \nu(\theta_1(t))$ we get the associated Legendre equation

$$(1-t^2)\frac{d}{dt}\left[(1-t^2)\frac{dP}{dt}\right] + \left[(1-t^2)\lambda - m^2\right] P = 0 \quad -1 \le t \le 1, \ m = 0, 1, 2, \ldots . \quad (1.13)$$

The associated Legendre Equation (1.13) has solutions that are bounded everywhere if and only if the eigenvalues λ are of the form, $\lambda_n = n(n+1), \quad n = 0, 1, 2, \ldots$. The eigenfunctions associated with such an eigenvalue λ_n are the Legendre functions P_n^m of degree n order m. Thus eigenvalues λ_n of (1.10) are $\lambda_n = n(n+1), \quad n = 0, 1, \ldots$ and the corresponding eigenfunctions are $S_n^m(\theta_1, \theta_2) = (A_m \cos m\theta_2 + B_m \sin m\theta_2) P_n^m(\cos\theta_1)$.

The weak formulation of (1.10) is, find $\lambda \in \mathbb{R}$, and $0 \neq \mu \in H^1(\mathbb{S})$ such that

$$a(\mu, \nu) = \lambda(\mu, \nu) \quad (1.14)$$

holds for every $\nu \in H^1(\mathbb{S})$, where $a(\cdot,\cdot) : H^1(\mathrm{S}) \times H^1(\mathrm{S}) \to \mathbb{R}$ is a continuous, elliptic bilinear form given by

$$a(\mu, \nu) = \int_{\mathrm{S}} \nabla_{\mathrm{S}}\mu \cdot \nabla_{\mathrm{S}}\nu.$$

The problem (1.14) has a sequence of eigenvalues,

$$\lambda_0 \le \lambda_{1,1} = \lambda_{1,2} = \lambda_{1,3} \le \ldots \le \lambda_{k,1} = \lambda_{k,2} = \ldots = \lambda_{k,2k+1} \le \ldots \to \infty,$$

and the corresponding eigenfunctions, which are spherical harmonics,

$$\mu_0, \mu_1, \ldots .$$

These eigenfunctions are orthogonal in the energy inner product

$$a_(\mu_i, \mu_j) = \lambda_i(\mu_i, \mu_j) = \lambda_i \delta_{ij},$$

where δ_{ij} is the Kronecker-delta function. Let μ with $\|\mu\|_a = 1$ denote an eigenfunction corresponding to λ and let $M(\lambda)$ denote the space of eigenfunctions corresponding to λ.

We are interested in approximating eigenvalues and eigenfunctions of (1.14) by the finite element method. We consider the following eigenvalue problem: Find $\lambda^h \in \mathbb{R}$ and $0 \neq \mu^h \in \chi$ such that

$$a_h(\mu^h, \nu^h) = \lambda^h(\mu^h, \nu^h) \tag{1.15}$$

for every $\nu^h \in \chi$ where χ is a finite dimensional subspace $\chi \subset H^1(\mathcal{S})$. Problem (1.15) has a sequence of eigenvalues,

$$\lambda_0^h \leq \lambda_1^h \leq \ldots \leq \lambda_n^h \quad n = \dim\chi$$

and corresponding eigenfunctions

$$\mu_0^h, \mu_1^h, \ldots, \mu_n^h$$

which are also orthogonal in the energy inner product.

$$a_(\mu_i^h, \mu_j^h) = \lambda_i(\mu_i^h, \mu_j^h) = \lambda_i \delta_{ij} \quad i, j = 1, \ldots n.$$

Let $\mu_{k,1}^h, \mu_{k,2}^h, \ldots, \mu_{k,2k+1}^h$ with $\|\mu_k^h\| = 1$ denote the finite element approximate eigenfunctions of $\lambda_{k,1}^h, \lambda_{k,1}^h, \ldots \lambda_{k,2k+1}^h$ respectively. The eigenpairs (λ^h, μ^h) of (1.15) are approximates of the eigenpairs (λ, μ) of (1.14). The eigenvalues λ_k and their approximates λ_k^h satisfy the following well-known minmax principles.

$$\lambda_k = \min_{U_k \subset H^1(\mathrm{S})} \max_{\mu \in S_k} \frac{a(\mu,\mu)}{(\mu,\mu)} \quad \lambda_k^h = \min_{S_k \subset X} \max_{\mu_h \in S_k} \frac{a(\mu_h,\mu_h)}{(\mu_h,\mu_h)}.$$

The minimum is taken over all k-dimensional subspaces, U_k, and S_k of $H^1(S)$, and X respectively. It follows immediately from the minmax principles that *every eigenvalue is approximated from above* by $2k+1$ of the approximated eigenvalues [5].

$$\lambda_k \leq \lambda_{k,1}^h \leq \lambda_{k,2}^h \leq \ldots \lambda_{k,2k+1}^h \quad \lambda_k \simeq \lambda_{k,1}^h, \lambda_{k,2}^h, \ldots \lambda_{k,2k+1}^h.$$

It is well known that,

$$\lambda_{k,q}^h - \lambda_k \leq C \sup_{\mu \in M(\lambda)} \inf_{\nu_h \in \chi} \|\mu - \nu_h\|_a \; q = 1, \ldots, 2k+1. \tag{1.16}$$

Here $\|\cdot\|_a$ denotes the energy norm [13],[14],[15].

Chapter 2

The Radial Projection

The aim of our work is to develop an exact finite element discretization of the sphere. This new method can be easily applied to other domains, e.g. cylinders, ellipsoids, and tori.

The principal idea behind our new method is to radially project the finite elements constructed on the surface of the cube onto the sphere. The cube is used as a tool in our approach, so that all the calculations are done on logically rectangular grids. We call these spherical triangles and the associated finite element functions formed by this radial projection as "radially projected finite elements". The radial projection is a mapping from the cube to the ball, or can be modified such that it is also a mapping from the surface of the cube (which we will call box) to the sphere, cylinder, ellipsoid, etc.

For definiteness we illustrate the method on the sphere. In order to make our terminology clearer, we will use box to indicate the surface of the cube. The relation between the box and the cube is similar to the relation between the sphere and the ball. We denote the sphere centered at the origin with radius r by $\mathcal{S}_r$ and the box centered at the origin with a side length $2d$ by $\mathcal{B}_d$. We denote points on the box by x and y and points on the sphere by a and b. Functions defined on $\mathcal{B}_d$ will be denoted by u or v, and similarly, functions defined on the $\mathcal{S}_r$ will be denoted by μ or ν. We now define the box $\mathcal{B}_d$, cube C_d, sphere $\mathcal{S}_r$, and ball B_r, to emphasize our terminology.

$$
\begin{aligned}
\mathcal{B}_d &= \{x = (x_1, x_2, \ldots, x_n) \in \mathbb{R}^n : \|x\|_\infty = d\}, \\
C_d &= \{x = (x_1, x_2, \ldots, x_n) \in \mathbb{R}^n : \|x\|_\infty \leq d\}, \\
\mathcal{S}_r &= \{a = (a_1, a_2, \ldots, a_n) \in \mathbb{R}^n : \|a\|_2 = r\}, \\
B_r &= \{a = (a_1, a_2, \ldots, a_n) \in \mathbb{R}^n : \|a\|_2 \leq r\},
\end{aligned}
$$

where $\|a\|_2 = \sqrt{a_1^2 + a_2^2 + \ldots + a_n^2}$ is the Euclidean norm and $\|x\|_\infty = \max(|x_1|, |x_2|, \ldots, |x_n|)$ is the maximum norm. Unless otherwise mentioned, hereinafter $\|\cdot\|$ will denote $\|\cdot\|_2$; and $\mathcal{S}$ will denote the unit sphere in $\mathbb{R}^3$ centered at the origin and $\mathcal{B}$ will denote the box in $\mathbb{R}^3$ with $d = 1$ centered at the origin.

The radial projection from a box to a sphere is denoted by $\mathcal{P} : \mathcal{B}_d \to \mathcal{S}_r$ and is given by

$$\mathcal{P}(x) = r\frac{x}{d\|x\|_2},$$

and the inverse projection is $\mathcal{P}^{-1} : \mathcal{S}_r \to \mathcal{B}_d$, is

$$\mathcal{P}^{-1}(a) = d\frac{a}{r\|a\|_\infty}.$$

In section 2.1 we list some properties of the radial projection and in section 2.2 we generate meshes on spheres, ellipsoids and cylinders.

2.1 Properties of the Radial Projection

The radial projection $\mathcal{P}$ is a one-to-one mapping from the box onto the sphere. In the following Lemma we show that both $\mathcal{P}$ and $\mathcal{P}^{-1}$ are *Lipschitz* continuous mappings.

Lemma 2.1 *The radial projection P and its inverse P^{-1} satisfy the inequalities*

$$\|P(x) - P(y)\| \leq \frac{2r}{\|x\|}\|x - y\| \tag{2.1}$$

and

$$\|P^{-1}(a) - P^{-1}(b)\|_\infty \leq \frac{2d}{\|a\|_\infty}\|a - b\|_\infty . \tag{2.2}$$

Proof:

$$\begin{aligned}
\|P(x) - P(y)\| &= \|\frac{r}{\|x\|}x - \frac{r}{\|y\|}y\| \\
&= \frac{r}{\|x\|\|y\|}\Big\|\|y\|x - \|x\|y\Big\| \\
&= \frac{r}{\|x\|\|y\|}\Big\|\|y\|(x-y) + y\Big(\|y\| - \|x\|\Big)\Big\| \\
&\leq \frac{r}{\|x\|\|y\|}\Big[\|y\|\|x-y\| + \|y\|\Big|\|y\| - \|x\|\Big|\Big] \\
&\leq \frac{2r}{\|x\|}\|x - y\|
\end{aligned}$$

Similary, $\|P^{-1}(a) - P^{-1}(b)\|_\infty \leq \frac{2d}{\|a\|_\infty}\|a - b\|_\infty$. □

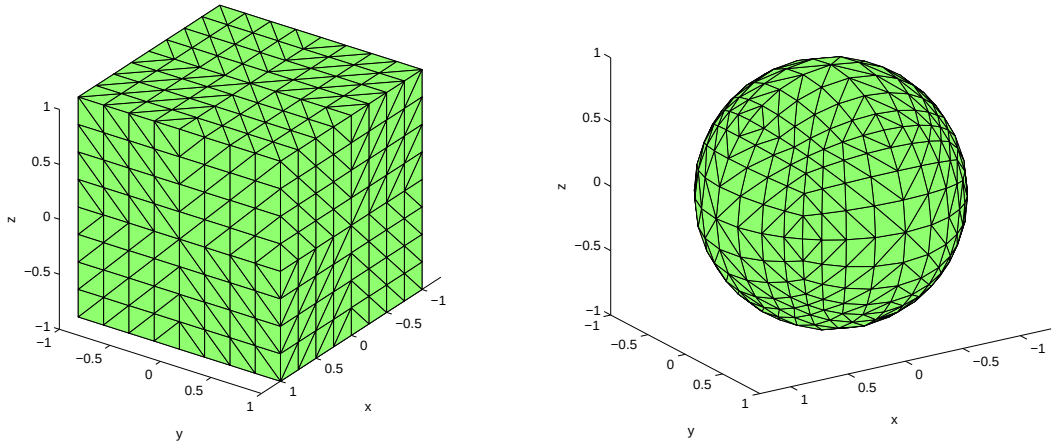

Figure 2.1: Mesh on the box and the sphere.

Corollary 2.1 *The radial projection P and its inverse P^{-1}, are globally Lipschitz continuous mappings,*

$$\|P(x) - P(y)\| \leq \frac{2r}{d}\|x - y\|, \tag{2.3}$$

and

$$\|P^{-1}(a) - P^{-1}(b)\| \leq 2dn\|a - b\|. \tag{2.4}$$

Proof: For any $x \in \mathbb{R}^n$, we have $\|x\|_\infty \leq \|x\| \leq \sqrt{n}\|x\|_\infty$, and for any $a \in \mathrm{S}$ we have $\frac{1}{\sqrt{n}} \leq \|a\|_\infty \leq 1$, and similarly, for any $x \in B$ $1 \leq \|x\| \leq \sqrt{n}$. Thus, the corollary is direct consequence of the lemma 2.1. □

2.2 Some Examples of Mapping

2.2.1 Mesh on the Sphere

Let $\mathcal{B}$ denote the box in $\mathbb{R}^3$ centered at the origin with side length 2, that is $\mathcal{B} = \{x = (x_1, x_2, x_3) \in \mathbb{R}^3 : \|x\|_\infty = 1\}$, and let $\mathcal{S}$ denote the unit sphere in $\mathbb{R}^3$ centered at the origin, that is $\mathcal{S} = \{a = (a_1, a_2, a_3) \in \mathbb{R}^3 : \|a\| = 1\}$. The mapping from the box $\mathcal{B}$ to the sphere $\mathcal{S}$ is given by,

$$\mathcal{P}(x) = \frac{x}{\|x\|},$$

and the inverse mapping from sphere $\mathcal{S}$ to $\mathcal{B}$ is,

$$\mathcal{P}^{-1}(a) = \frac{a}{\|a\|_\infty}.$$

Figure 2.1 shows the finite element triangulation on $\mathcal{B}$ and the corresponding triangulation on $\mathcal{S}$. We can think of the box, $\mathcal{B}$, as a union of 6 faces. Let $\mathcal{F}_{\pm i}$, $i = 1 \ldots 3$ denote the faces of the box such that, $\mathcal{F}_{+i}$ corresponds to the $x_i = 1$ plane, and $\mathcal{F}_{-i}$ corresponds to the $x_i = -1$ plane. Since on each face one of the variables is constant, the mesh generation on these faces is the same as mesh generation on a 2-dimension planar square. The radial projection of any of these faces $\mathcal{F}_{\pm i}\, i = 1 \ldots 3$ onto the sphere is given as

$$\mathcal{P}_{\mathcal{F}_{\pm i}}(x_1, x_2, x_3) = \left(\frac{x_1}{\sqrt{x_1^2 + x_2^2 + x_3^2}}, \frac{x_2}{\sqrt{x_1^2 + x_2^2 + x_3^2}}, \frac{x_3}{\sqrt{x_1^2 + x_2^2 + x_3^2}} \right) \; i = 1, \ldots, 3$$

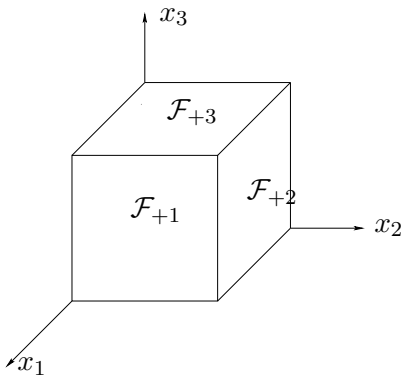

Figure 2.2: Faces of the box

and the inverse projection onto these faces are given as

$$\begin{aligned}
\mathcal{P}^{-1}_{\mathcal{F}_{\pm 1}}(a_1, a_2, a_3) &= \left(\pm 1, \pm\frac{a_2}{a_1}, \pm\frac{a_3}{a_1}\right), \\
\mathcal{P}^{-1}_{\mathcal{F}_{\pm 2}}(a_1, a_2, a_3) &= \left(\pm\frac{a_1}{a_2}, \pm 1, \pm\frac{a_3}{a_2}\right), \\
\mathcal{P}^{-1}_{\mathcal{F}_{\pm 3}}(a_1, a_2, a_3) &= \left(\pm\frac{a_1}{a_3}, \pm\frac{a_2}{a_3}, \pm 1\right).
\end{aligned}$$

Figure 2.3 and 2.4 show the triangulation on $\mathcal{F}_{+1}$ and its radial projection onto the sphere.

Let $\mathcal{K} = \{\mathcal{K}_1, \mathcal{K}_2, \ldots, \mathcal{K}_n\}$ be a triangulation of the box, then $\mathcal{T} = \mathcal{P}(\mathcal{K})$, is a triangulation of the sphere. Let $\mathcal{T} = \{\mathcal{T}_1, \mathcal{T}_2, \ldots, \mathcal{T}_n\}$ denote the corresponding triangulation of the sphere where $\{\mathcal{T}_i : \mathcal{T}_i = \mathcal{P}(\mathcal{K}_i),\ i = 1, \ldots, n\}$ are the spherical triangles covering the sphere, such that $\mathcal{S} = \bigcup_{i=1}^{n} \mathcal{T}_i$.

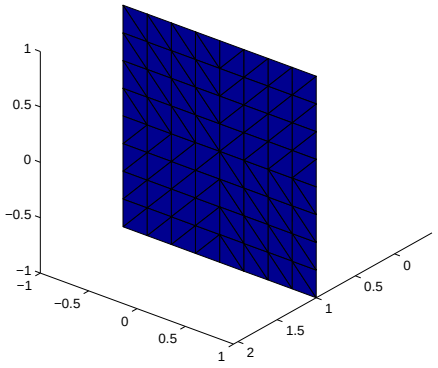

Figure 2.3: $\mathcal{F}_{+1}$.

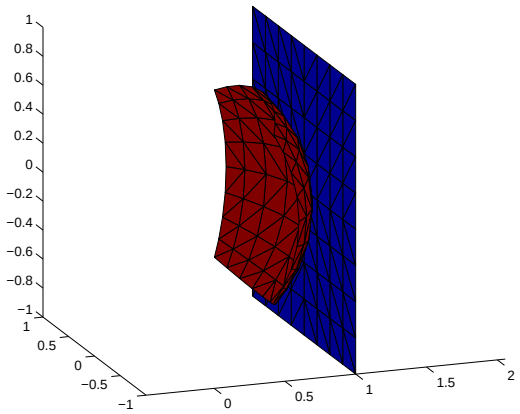

Figure 2.4: $\mathcal{F}_{+1}$ and $\mathcal{P}\left(\mathcal{F}_{+1}\right)$.

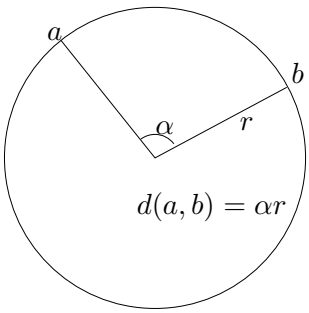

Figure 2.5: Geodesic distance between a and b.

We measure the distance between two points on the sphere by the geodesic distance. Let a and b be two points on $\mathcal{S}_r$, then the geodesic distance is defined by

$$d(a,b) = r\cos^{-1}(\frac{a\cdot b}{r^2}). \tag{2.5}$$

The geodesic distance between two points, a and b on a sphere is the length of the arc of the great circle connecting them. This great circle lies on a plane, figure 2.5 shows a 2D cross section of the sphere. Let α be the angle between a, the center of the sphere O and b as shown in the figure, then $d(a,b) = \alpha r$.

Proposition 2.1 *Let a and b be two distinct points on the unit sphere centered at the origin in $\mathbb{R}^3$, then we have the following estimate,*

$$\frac{1}{2}d(a,b) \leq \|a-b\| \leq d(a,b). \tag{2.6}$$

Proof: The geodesic distance between a and b is $d(a,b) = \alpha$, which is the distance along the great circle connecting them. Figure (2.6) shows that $\|a-b\| = 2\sin\left(\frac{\alpha}{2}\right)$. Clearly,

$$\frac{\|a-b\|}{d(a,b)} = \frac{2\sin\left(\frac{\alpha}{2}\right)}{\alpha}.$$

Let $f(\alpha) = \frac{2\sin\left(\frac{\alpha}{2}\right)}{\alpha}$, then $f'(\alpha) = \frac{\alpha\cos\left(\frac{\alpha}{2}\right) - 2\sin\left(\frac{\alpha}{2}\right)}{\alpha^2}$. The function f is a decreasing function on the interval $\alpha \in [0,\pi]$, since $f'(\alpha) < 0$ $\alpha \in (0,\pi)$ which is equivalent to $x - \tan(x) < 0$ $x \in (0,\pi/2)$. Clearly, $f(\alpha)$ has a maximum at $\alpha = 0$, $f(0) = 1$ and a minimum at $\alpha = \pi$, $f(\pi) = \frac{2}{\pi}$, that is $\frac{1}{2} \leq \frac{\|a-b\|}{d(a,b)} \leq 1$. □

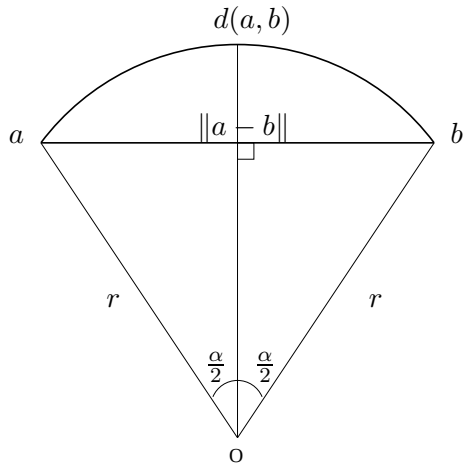

Figure 2.6: Geodesic and Euclidean distance of a and b

With the following proposition, we prove that radially projected finite elements form a shape regular triangulation of the sphere.

Proposition 2.2 *Let $\mathcal{T}^j,\ j \in \mathbb{N}$ denote the family of triangulations of the sphere $\mathcal{S}$, and let $\mathcal{K}^j,\ j \in \mathbb{N}$ denote the family of triangulations of the box B, such that $\mathcal{P}(\mathcal{K}^j) = \mathcal{T}^j$. If $\mathcal{K}^j$ is a shape regular triangulation of $\mathcal{B}$, then $\mathcal{T}^j$ is a shape regular triangulation of $\mathcal{S}$.*

Proof: Let $\mathcal{T}^j = \{\mathcal{T}_1, \mathcal{T}_2, \ldots, \mathcal{T}_{n_j}\}$, $j \in \mathbb{N}$ denote the triangulation of the sphere and let $\mathcal{K}^j = \{\mathcal{K}_1, \mathcal{K}_2, \ldots, \mathcal{K}_{n_j}\}$, $j \in \mathbb{N}$ be a triangulation of the box such that $P(\mathcal{K}_i) = \mathcal{T}_i$, $i = 1, \ldots, n_j$. Let a and b be two points on the sphere such that $h_{T_i} = d(a,b)$. Since $d(a,b) \leq 2\|a-b\| \leq 2\|x-y\|$, where $x = P^{-1}(a)$ and $y = P^{-1}(b)$ we get that $h_{\mathcal{T}_i} \leq 2h_{\mathcal{K}_i}$. Similarly, let $\rho_{\mathcal{K}_i}$ denote the radius of inscribed circle in the triangle $\mathcal{K}_i$ and consider two points x and y in the triangle $\mathcal{K}_i$, such that $\rho_{\mathcal{K}_i} = \|x-y\|$. Let a and b be two pints on the sphere such that $a = P(x)$ and $b = P(y)$, then $\rho_{\mathcal{T}_i} \geq d(a,b)$. Since, $d(a,b) \geq \|a-b\| \geq \frac{1}{6}\|x-y\|$, we conclude that $\rho_{\mathcal{T}_i} \geq \frac{1}{6}\rho_{\mathcal{K}_i}$. □

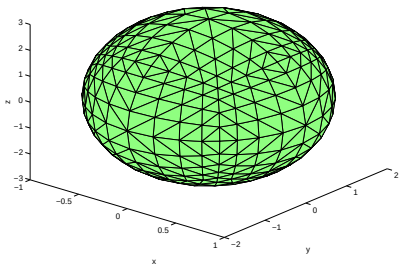

Figure 2.7: Mesh on the ellipsoid

2.2.2 Meshes on Ellipsoids

Let $\mathcal{B}$ denote the box in $\mathbb{R}^3$ with side length 2, that is $\mathcal{B} = \{x \in R^3 : \|x\|_\infty = 1\}$, and let $\mathcal{S}$ denote the sphere in $\mathbb{R}^3$ with radius 1, that is $\mathcal{S} = \{a \in R^3 : \|a\| = 1\}$ and let $\mathcal{E}$ denote the ellipsoid in $\mathbb{R}^3$ such that $\mathcal{E} = \{b = (b_1, b_2, b_3) \in R^3 : \frac{b_1^2}{k^2} + \frac{b_2^2}{l^2} + \frac{b_3^2}{m^2} = 1\}$. The mapping $\mathcal{M}$ from box $\mathcal{B}$ to ellipsoid $\mathcal{E}$ is the composition of the radial projection $\mathcal{P}$ of $\mathcal{B}$ onto sphere $\mathcal{S}$ with the linear mapping $\mathcal{L}$ from sphere $\mathcal{S}$ to the ellipsoid $\mathcal{E}$. The mapping $\mathcal{L} : \mathcal{S} \to \mathcal{E}$ is given as

$$\mathcal{L}(a) = (ka_1, la_2, ma_3)\,,$$

thus $\mathcal{M} : \mathcal{B} \to \mathcal{E}$ is

$$\mathcal{M}(x) = \left(\frac{k\|x\|_\infty}{\|x\|}x_1, \frac{l\|x\|_\infty}{\|x\|}x_2, \frac{m\|x\|_\infty}{\|x\|}x_3\right),$$

and $\mathcal{M}^{-1} : \mathcal{E} \to \mathcal{B}$ is

$$\mathcal{M}^{-1}(b) = \left(1, \frac{kb_2}{lb_1}, \frac{kb_3}{mb_1}\right),$$

if $\|\mathcal{L}^{-1}(b)\|_\infty = \frac{b_1}{k}$.

Let $\mathcal{K} = \{\mathcal{K}_1, \mathcal{K}_2, \ldots, \mathcal{K}_n\}$ be the triangulation of the box, then $\mathcal{T} = \mathcal{M}(\mathcal{K})$, is the triangulation of the ellipsoid. Let $\mathcal{T} = \{\mathcal{T}_1, \mathcal{T}_2, \ldots, \mathcal{T}_n\}$ denote the corresponding triangulation of the ellipsoid where $\{\mathcal{T}_i : \mathcal{T}_i = \mathcal{M}(\mathcal{K}_i),\ i = 1, \ldots, n\}$ are the triangles covering the ellipsoid, such that $\mathcal{E} = \bigcup_{i=1}^{n} \mathcal{T}_i$.

2.2.3 Mesh on the Cylinder

Let $\mathcal{B}$ denote the surface of the cube in $\mathbb{R}^3$ with side length 2 and centered at the origin, that is $\mathcal{B} = \{x \in R^3 : \|x\|_\infty = 1\}$, and let $\mathcal{C}$ denote the surface of the circular right cylinder in $\mathbb{R}^3$ of height 2 and radius 1. By cylinder we mean the following: $\mathcal{C} = \{a = (a_1, a_2, a_3),\ a \in R^3 : a_1^2 + a_2^2 = 1,\ -1 < a_3 < 1,\ \text{ and } a_1^2 + a_2^2 \leq 1, a_3 = \pm 1\}$. In other words it is a cylinder with top and bottom faces. The mapping from box $\mathcal{B}$ to sphere $\mathcal{C}$ is given by,

$$\mathcal{P}(x) = \left(\frac{\|x\|_\infty}{\|x\|} x_1, \frac{\|x\|_\infty}{\|x\|} x_2, x_3 \right).$$

and the inverse mapping from the cylinder $\mathcal{C}$ to the box $\mathcal{B}$ is given by,

$$\mathcal{P}^{-1}(a) = \left(\frac{\|a\|}{\|a\|_\infty} a_1, \frac{\|a\|}{\|a\|_\infty} a_2, a_3 \right).$$

Let $\mathcal{K} = \{\mathcal{K}_1, \mathcal{K}_2, \ldots, \mathcal{K}_n\}$ be the triangulation of the box, then $\mathcal{T} = \mathcal{P}(\mathcal{K})$, is the triangulation of the cylinder. Let $\mathcal{T} = \{\mathcal{T}_1, \mathcal{T}_2, \ldots, \mathcal{T}_n\}$ denote the corresponding triangulation of the cylinder where $\{\mathcal{T}_i : \mathcal{T}_i = \mathcal{P}(\mathcal{K}_i),\ i = 1, \ldots, n\}$ are the triangles covering the cylinder, such that $\mathcal{C} = \bigcup_{i=1}^{n} \mathcal{T}_i$. One may also prove that, mesh generated on the cylinder in such way, is also a shape regular mesh.

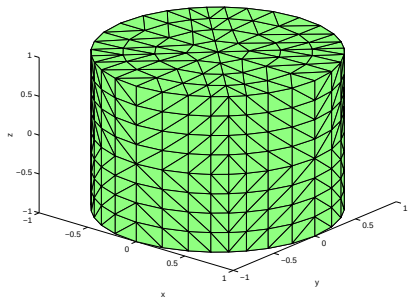

Figure 2.8: Mesh on the cylinder

2.2.4 Mesh on the Disc

Let B denote the square in $\mathbb{R}^2$ such that $B = \{x = (x_1, x_2) \in \mathbb{R}^2 : \|x\|_\infty \leq 1\}$, and let D denote the unit disc in $\mathbb{R}^2$, such that $D = \{a = (a_1, a_2) \in \mathbb{R}^2 : \|a\| \leq 1\}$, then the mapping from the square B to the unit disc D is given by

$$\mathcal{P}(x) = \frac{\|x\|_\infty}{\|x\|} x$$

and the inverse mapping is given as

$$\mathcal{P}^{-1}(a) = \frac{\|a\|}{\|a\|_\infty} a.$$

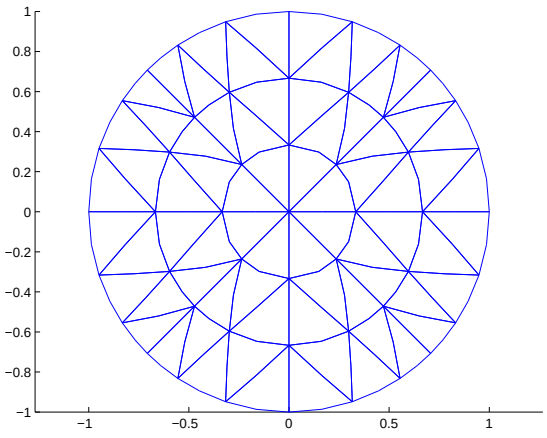

Figure 2.9: Mesh on the disc

Chapter 3

Analysis

In this chapter, we consider the problem of determining error estimates in L^2 and H^1 norms. We estimate the difference $(\mu - \mu_h)$ where μ is the solution of a second order elliptic problem and μ_h is the discrete solution obtained using the proposed finite element method. In section (3.1) we analyze our finite element discretization and in section (3.2) we derive error estimates.

3.1 Finite Element Construction

We describe our method in the context of the Laplace-Beltrami equation defined on the sphere $\mathcal{S}$. We consider the following second order elliptic equation on the sphere,

$$-\Delta_{\mathcal{S}}\mu + \mu = f, \tag{3.1}$$

where $-\Delta_{\mathcal{S}}$ is the Laplace-Beltami operator

$$\Delta_{\mathcal{S}} = \nabla_{\mathcal{S}} \cdot \nabla_{\mathcal{S}}.$$

Here $\nabla_{\mathcal{S}}$ is the tangential gradient which is defined as

$$\nabla_{\mathcal{S}}\mu = \nabla\tilde{\mu} - (\nabla\tilde{\mu} \cdot n)n$$

where n is the unit outer normal to the sphere at the point a and $\tilde{\mu}$ is a smooth extension of μ to a neighborhood of $\mathcal{S}$. Since $\mathcal{S}$ is a smooth compact manifold without boundary, there are no boundary conditions needed.

We use the standard notation $L^p(\mathcal{S})$, $W^{m,p}(\mathcal{S})$ for Sobolev spaces defined on the sphere.

$$\begin{aligned} L^p(\mathcal{S}) &= \{\mu : \int_{\mathcal{S}} |\mu|^p < \infty\} \\ W^{m,p}(\mathcal{S}) &= \{\mu \in L^p(\mathcal{S}) : \int_{\mathcal{S}} |\nabla^\alpha_{\mathcal{S}}\mu|^p < \infty \text{ , for } 0 < |\alpha| \leq m\}, \end{aligned}$$

where $\alpha = (\alpha_1, \alpha_2, \alpha_3)$ is a multi index notation with norm $|\alpha| = \alpha_1 + \alpha_2 + \alpha_3$. $W^{m,p}(\mathcal{S})$ is a Banach space equipped with the norm

$$\|\mu\|_{W^{m,p}(\mathcal{S})} = \left(\sum_{0<|\alpha|\leq m} \|\nabla^\alpha_{\mathcal{S}}\mu\|^p_{L^p(\mathcal{S})} \right)^{\frac{1}{p}} \quad 1 \leq p < \infty.$$

Let $H^m(\mathcal{S})$ denote $W^{m,2}(\mathcal{S})$, then the semi-norms on $H^m(\mathcal{S})$ are $|\mu|_{H^m(\mathcal{S})} = \left(\sum_{|\alpha|=m} \|\nabla^\alpha_{\mathcal{S}}\mu\|^2_{L^2(\mathcal{S})} \right)^{\frac{1}{p}}$. Let $f \in L^2(\mathcal{S})$, then there exist an exact solution $\mu \in H^2(\mathcal{S})$ to (3.1). There exist a constant c, such that[16],

$$\|\mu\|_{H^2(\mathcal{S})} \leq c\|f\|_{L^2(\mathcal{S})}.$$

A weak formulation of (3.1): find a solution $\mu \in H^1(\mathcal{S})$ such that the following holds,

$$\int_S \nabla_{\mathcal{S}}\mu \cdot \nabla_{\mathcal{S}}\nu + \mu \cdot \nu = \int_{\mathcal{S}} f \cdot \nu \quad \forall \nu \in H^1(\mathcal{S}). \tag{3.2}$$

Let $f \in L^2(\mathcal{S})$ and $\mu \in H^2(\mathcal{S})$, then μ is a solution of (3.2) iff μ is a solution of (3.1). Let $a(\cdot,\cdot) : H^1(\mathcal{S}) \times H^1(\mathcal{S}) \to \mathbb{R}$ be the bilinear form defined by

$$a(\mu,\nu) := \int_S \nabla_{\mathcal{S}}\mu \cdot \nabla_{\mathcal{S}}\nu + \mu \cdot \nu. \tag{3.3}$$

Notice that $a(\cdot,\cdot)$ is continuous, elliptic bilinear form, since $\|\mu\|_{H^1(\mathcal{S})} = \sqrt{a(\mu,\mu)}$, and

$$(f,\nu) := \int_{\mathcal{S}} f \cdot \nu$$

is the standard inner product in $L^2(\mathcal{S})$.

Theorem 3.1 *There exists a unique solution to (3.2).*

Proof: The symmetric, elliptic bilinear form $a(\cdot,\cdot)$ (3.3) induces a norm on $H^1(\mathcal{S})$. The space $(H^1(\mathcal{S}), a(\cdot,\cdot))$ is a Hilbert space, so the conclusion is a direct consequence of the Riesz Representation theorem. □

We approximate the solution μ by $\mu_h \in \chi$, where χ is in a finite dimensional subspace of $H^1(\mathcal{S})$. We solve the following discrete problem:

$$\text{find a function } \mu_h \in \chi \text{ such that } \int_S \nabla_{\mathcal{S}}\mu_h \cdot \nabla_{\mathcal{S}}\nu_h + \mu_h \cdot \nu_h = \int_{\mathcal{S}} f \cdot \nu_h \quad \forall \nu_h \in \chi. \tag{3.4}$$

Let $a_h(\cdot,\cdot) : \chi \times \chi \to \mathbb{R}$ denote the bilinear form defined as

$$a_h(\mu_h,\nu_h) := \int_S \nabla_{\mathcal{S}}\mu_h \cdot \nabla_{\mathcal{S}}\nu_h + \mu_h \cdot \nu_h,$$

and let $(f,\cdot):\chi\to\mathbb{R}$ denote the linear functional defined as $(f,\nu_h):=\int_{\mathcal{S}} f\cdot\nu_h$, then the discrete problem is: find $\mu_h\in\chi$ such that $a_h(\mu_h,\nu_h)=(f,\nu_h)$ for every $\nu_h\in\chi$. Define χ as

$$\chi=\{\mu_h:\ \mu_h=u\circ P^{-1},\ \text{u is a piecewise linear continuous polynomial}\}. \tag{3.5}$$

This dicrete problem has a unique solution. Since χ is a finite dimensional subspace of $H^1(\mathcal{S})$, let $\{\varphi_i\}_{i=1}^n$ be a basis for χ. Letting $\mu_h=\sum_{i=1}^{n}\mu_{hi}\varphi_i$, leads to following linear system of equations

$$A\mu=f. \tag{3.6}$$

Here, $A_{ij}=a(\varphi_j,\varphi_i)$ is a sparse, symmetric, positive definite matrix, $(\mu)_i=\mu_{hi}$ is the unknown vector, $(f)_i=(f,\varphi_i)$ is the right hand side vector.

3.2 Error Analysis

Let μ be the solution of (3.2) and μ_h be the solution of (3.4). We want to get an error estimate of the form,

$$\|\mu-\mu_h\|_{H^k(\mathcal{S})}\le ch^p,\quad k=0,1,$$

where p is the order of convergence for the method and depends on the the regularity of the solution, degree of the finite elements used (on the planar triangles in the construction of the finite elements) and the Sobolev norm used to measure the error.

If we let $T=\{\mathcal{K}_1,\mathcal{K}_2,\ldots,\mathcal{K}_n\}$ denote the partition of the sphere, such that $\mathcal{S}=\cup_{i=1}^{n}\mathcal{K}_i$, then

$$\|\mu\|_{H^k(\mathcal{S})}=\left(\sum_{i=1}^{n}\|\mu\|^2_{H^k(\mathcal{K}_i)}\right)^{1/2}.$$

Cea's Lemma has a significant role in describing error estimates in finite element analysis, since it reduces the problem of estimating the error $\|\mu - \mu_h\|_{H^1(\mathcal{S})}$ to a problem of estimating the distance between the function $\mu \in H^1(\mathcal{S})$ and a function μ_h in its subspace $\chi \subset H^1(\mathcal{S})$. By Cea's Lemma we know that

$$\|\mu - \mu_h\|_{H^1(\mathcal{K})} \leq C \inf_{\xi \in \chi} \|\mu - \xi\|_{H^1(\mathcal{K})}.$$

Thus, μ_h is the best approximation of μ with respect to H^1-norm within the space χ. We can replace ξ on right hand side by the interpolant of the exact solution $\mathcal{I}\mu$ and we get,

$$\|\mu - \mu_h\|_{H^1(\mathcal{K})} \leq C\|\mu - \mathcal{I}\mu\|_{H^1(\mathcal{K})}.$$

We wish to consider the size of the error in $\|\mu - \mu_h\|_{L^2(\mathcal{K})}$. To estimate the error $\mu - \mu_h$ in L^2-norm, we use so called "duality" argument thus,

$$\|\mu - \mu_h\|_{L^2(\mathcal{K})} \leq Ch\|\mu - \mu_h\|_{H^1(\mathcal{K})}.$$

Therefore, rather than estimating the difference $\|\mu - \mu_h\|_{L^2(\mathcal{K})},\ \|\mu - \mu_h\|_{H^1(\mathcal{K})}$, we will be estimating $\|\mu - \mathcal{I}\mu\|_{L^2(\mathcal{K})},\ \|\mu - \mathcal{I}\mu\|_{H^1(\mathcal{K})}$.

Consider a spherical triangle $\mathcal{K}$ in $\mathcal{T}$ and consider a planar triangle $\mathcal{K}_h$ such that for every $x \in \mathcal{K}_h$ $\frac{x}{\|x\|} \in \mathcal{K}$. In other words, $\mathcal{K}$ is the radial projection of $\mathcal{K}_h$ onto the sphere, i.e., $\mathcal{P}(\mathcal{K}_h) = \mathcal{K}$. Moreover, suppose that the spherical triangle, $\mathcal{K}$, and the planar triangle $\mathcal{K}_h$ share the same nodes. Figure (3.1) shows the planar triangle $\mathcal{K}_h$ and the spherical triangle $\mathcal{K}$. The union of the spherical triangles covers the sphere, and the union of planar triangles

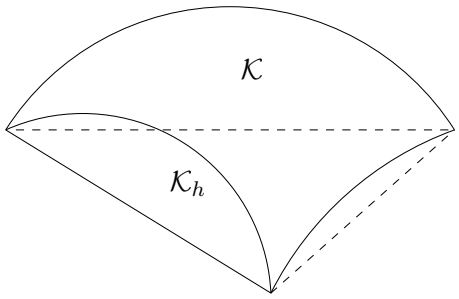

Figure 3.1: Spherical triangle, $\mathcal{K}$ and planar triangle $\mathcal{K}_h$.

forms a polygonal surface Ω, i.e.,

$$\mathcal{S} = \cup_{i=1}^{n} \mathcal{K}_i \text{ and } \Omega = \cup_{i=1}^{n} \mathcal{K}_{h_i}.$$

If $\{\eta_i\}_{i=1}^{m}$ denote the nodes of spherical triangles covering the sphere, then $\Omega \cap \mathcal{S} = \{\eta_i\}_{i=1}^{m}$.

Define $U = \{x = (x_1, x_2, x_3) \in \mathbb{R}^3 : \frac{1}{2} \leq \|x\| \leq \frac{3}{2}\}$, so that both $\mathcal{K} \subset U,$ and $\mathcal{K}_h \subset U$, then we may extend a function μ defined on the $\mathcal{S}$ uniquely to the three dimensional domain U by

$$E\mu(x) = \mu(\frac{x}{\|x\|}) \quad \text{for every } x \in U. \tag{3.7}$$

Clearly $E\mu(a) = \mu(a)$ if $a \in \mathcal{S}$ and note that $E\mu$ is constant along the normal direction to the sphere, that is $E\mu$ does not depend on r, if spherical coordinates are used, so

$$\nabla E\mu \cdot n = 0,$$

where $n = (a_1, a_2, a_3)$ is the normal to the sphere $\mathcal{S}$ at the point a.

The tangential gradient of the real valued function μ on $\mathcal{S}$ is the orthogonal projection of the gradient of μ onto the tangent plane at the point a. Let $n = (a_1, a_2, a_3)$ denote the unit outward normal at the point a on $\mathcal{S}$, then tangential gradient, $\nabla_{\mathcal{S}}\mu = \nabla E\mu - (\nabla E\mu \cdot n)\, n$, can be expressed as:

$$\nabla_{\mathcal{S}}\mu = A\nabla\mu \tag{3.8}$$

where A is the 3×3 matrix matrix with

$$(A)_{ij} = \begin{cases} 1 - a_i^2 & i = j \\ a_i a_j & i \neq j. \end{cases} \tag{3.9}$$

Since $\nabla_{\mathcal{S}}\mu$ is the projection of $\nabla\mu$ on to the tangent plane, $\nabla_{\mathcal{S}}\mu \cdot n = 0$, we have

$$\|\nabla_{\mathcal{S}}\mu\|^2 = \|\nabla\mu\|^2 - |n \cdot \nabla\mu|^2.$$

Thus, $\|\nabla_{\mathcal{S}}\mu\| \leq \|\nabla\mu\|$.

Proposition 3.1 *We have the following identities for the second order tangential derivatives of* μ

$$\nabla^2_{\mathcal{S}}\mu \;=\; \nabla\left(\nabla_{\mathcal{S}}\mu\right) + \nabla_{\mathcal{S}}\mu n, \tag{3.10}$$

and

$$\nabla^2_{\mathcal{S}}\mu n \;=\; A\nabla_{\mathcal{S}}\mu, \tag{3.11}$$

where A is given in (3.9). Note that unlike the Hessian, $\nabla^2_{\mathcal{S}}\mu$ is not symmetric.

Proof: Since

$$a_1\nabla_{\mathcal{S},1}\mu + a_2\nabla_{\mathcal{S},2}\mu + a_3\nabla_{\mathcal{S},3}\mu = 0, \tag{3.12}$$

taking the gradient of both sides of (3.12), we have

$$a_1 D_i\nabla_{\mathcal{S},1}\mu + a_2 D_i\nabla_{\mathcal{S},2}\mu + a_3 D_i\nabla_{\mathcal{S},3}\mu = -D_i\nabla_{\mathcal{S}_i}\mu \quad i = 1,2,3. \tag{3.13}$$

(3.10) is direct consequence of (3.13). Let ν be a real valued function differentiable at $a \in \mathcal{S}$, then $\nabla_{\mathcal{S}}(\mu\nu) = \mu\nabla_{\mathcal{S}}\nu + \nu\nabla_{\mathcal{S}}\mu$. Taking tangential derivative of both sides of (3.12), we get

$$a_1\nabla_{\mathcal{S}}(\nabla_{\mathcal{S},1}\mu) + a_2\nabla_{\mathcal{S}}(\nabla_{\mathcal{S},2}\mu) + a_3\nabla_{\mathcal{S}}(\nabla_{\mathcal{S},3}\mu) = -\nabla_{\mathcal{S}}a_1\nabla_{\mathcal{S}}\mu + \nabla_{\mathcal{S}}a_2\nabla_{\mathcal{S}}\mu + \nabla_{\mathcal{S}}a_3\nabla_{\mathcal{S}}\mu$$

Since, $\nabla_{\mathcal{S}}a_1 = \begin{pmatrix} 1-a_1^2 \\ -a_1a_2 \\ -a_1a_3 \end{pmatrix}$, $\nabla_{\mathcal{S}}a_2 = \begin{pmatrix} -a_1a_2 \\ -1-a_2^2 \\ -a_2a_3 \end{pmatrix}$, and $\nabla_{\mathcal{S}}a_3 = \begin{pmatrix} -a_3a_1 \\ -a_3a_2 \\ 1-a_3^2 \end{pmatrix}$, from which (3.11) follows immediately. □

Proposition 3.2 *Let $E\mu : U \to \mathbb{R}$ be defined by (3.7) for $x \in U$, let $a = \frac{x}{\|x\|} \in \mathcal{S}$ then we have the following identities;*

$$\nabla_{\mathcal{S}}\mu = \nabla_a E\mu, \tag{3.14}$$

$$\nabla_x E\mu = \frac{1}{\|x\|}\nabla_{\mathcal{S}}\mu, \tag{3.15}$$

$$\nabla_x(\nabla_{\mathcal{S}}\mu) = \frac{1}{\|x\|}A\nabla_a(\nabla_{\mathcal{S}}\mu), \tag{3.16}$$

$$\nabla^2_{\mathcal{S}}\mu = A\nabla_a(\nabla_{\mathcal{S}}\mu). \tag{3.17}$$

Here $\nabla_x = (D_{x_1}, D_{x_2}, D_{x_3})$ denotes the ordinary gradient with respect to the variable x and similarly $\nabla_a = (D_{a_1}, D_{a_2}, D_{a_3})$ denotes the ordinary gradient with respect to the variable a.

Proof: For any $a \in \mathcal{S}$, we have

$$\nabla_{\mathcal{S}}\mu(a) = \nabla_{\mathcal{S}}E\mu(a) = \nabla_a E\mu(a) - (\nabla_a E\mu(a) \cdot n)\, n = \nabla_a E\mu(a).$$

Since $E\mu(x) = E\mu(\frac{x}{\|x\|})$, by applying the chain rule we get,

$$\frac{\partial E\mu}{\partial x_i} = \frac{\partial E\mu}{\partial a_1}\frac{\partial a_1}{\partial x_i} + \frac{\partial E\mu}{\partial a_2}\frac{\partial a_2}{\partial x_i} + \frac{\partial E\mu}{\partial a_3}\frac{\partial a_3}{\partial x_i} \quad i = 1, 2, 3.$$

So,

$$\nabla_x E\mu(x) = J^T \nabla E\mu(a), \tag{3.18}$$

where J^T is the transpose of Jacobian matrix of the projection $\mathcal{P}(x) = \frac{x}{\|x\|}$ and,

$$J^T = \begin{pmatrix} \frac{1}{\|x\|} - \frac{x_1^2}{\|x\|^3} & -\frac{x_1 x_2}{\|x\|^3} & -\frac{x_1 x_3}{\|x\|^3} \\ -\frac{x_2 x_1}{\|x\|^3} & \frac{1}{\|x\|} - \frac{x_2^2}{\|x\|^3} & -\frac{x_2 x_3}{\|x\|^3} \\ -\frac{x_3 x_1}{\|x\|^3} & -\frac{x_3 x_2}{\|x\|^3} & \frac{1}{\|x\|} - \frac{x_3^2}{\|x\|^3} \end{pmatrix} = \frac{1}{\|x\|} A$$

Thus $\nabla_x E\mu(x) = \frac{1}{\|x\|}\nabla_{\mathcal{S}}\mu(a)$.

Since $D_{x_1}E\mu = \frac{1}{\|x\|}D_{a_1}E\mu(a)$ and $a = \mathcal{P}(x)$, by chain rule we have the following

$$D_{x_i}\left(D_{a_j}E\mu(a)\right) = D_{a_1}(D_{a_j}E\mu)\frac{\partial a_1}{\partial x_i} + D_{a_2}(D_{a_j}E\mu)\frac{\partial a_2}{\partial x_i} + D_{a_3}(D_{a_j}E\mu)\frac{\partial a_3}{\partial x_i}\; i, j = 1, 2, 3. \tag{3.19}$$

In matrix form, (3.19) and (3.16) are the same. Applying the tangential gradient twice to the real valued function μ we get (3.17). $\square$

Let χ_h denote the finite element space on a polygonal domain, Ω, consisting of piecewise linear continuous functions, i.e;

$$\chi_h = \{v : v \text{ is piecewise linear continuous polynomial}\}.$$

Let $\{\phi_i\}_{i=1}^n$ be basis for χ_h, such that $\phi_i(\eta_j) = \delta_{ij}$ where δ_{ij} is the Kronecker-delta. Let χ be the finite element space in (3.5), define $\varphi_i = \phi_i \circ \mathcal{P}^{-1},\ i = 1, \ldots, n$, then $\{\varphi_i\}_{i=1}^n$ is a basis for χ.

For any piecewise linear function v on Ω, we have

$$v(x) = \sum_{i=1}^{n} c_i \phi(x) \quad x \in \Omega \subset U$$

thus,

$$\mu(a) = \sum_{i=1}^{n} c_i \varphi(a) = \sum_{i=1}^{n} c_i \phi(\mathcal{P}^{-1}(a)) \quad a \in \mathcal{S}.$$

Let $E\mu$ be defined by (3.7), then $E\mu(x) = v(x), \quad x \in \Omega$. Clearly, if $x \in \mathcal{K}_h$, then $a = \frac{x}{\|x\|} \in \mathcal{K}$.

Lemma 3.1 *Let μ and v be real valued functions, then for some constants $c_i,\ i = 1, \ldots, 5$ we have the following relations for the equivalence of norms,*

$$c_1 \|v\|_{L^2(\mathcal{K}_h)} \leq \|\mu\|_{L^2(\mathcal{K})} \leq c_2 \|v\|_{L^2(\mathcal{K}_h)}$$

$$c_3 \|v\|_{H^1(\mathcal{K}_h)} \leq \|\mu\|_{H^1(\mathcal{K})} \leq c_4 \|v\|_{H^1(\mathcal{K}_h)}$$

$$|v|_{H^2(\mathcal{K}_h)} \leq c_5 \|\mu\|_{H^2(\mathcal{K})}.$$

Proof: Let J denote the Jacobian matrix of the projection $\mathcal{P}$, then there exists constants $c_1 > 0,\ c_2 > 0$ such that $|J| \leq c_1$ and $|J^{-1}| \leq \frac{1}{c_2}$.Thus

$$\begin{aligned} \|\mu\|^2_{L^2(\mathcal{K})} &= \int_{\mathcal{K}} |\mu|^2 \\ &= \int_{\mathcal{K}_h} |\mu \circ \mathcal{P}|^2 |J| \\ &\leq c_1 \int_{\mathcal{K}_h} |v|^2 \\ &= c_1 \|v\|^2_{L^2(\mathcal{K}_h)}. \end{aligned}$$

Similarly,

$$\|v\|^2_{L^2(K_h)} \leq \frac{1}{c_2} \|\mu\|^2_{L^2(K)}.$$

For any $x \in \mathcal{K}_h$, there exists constants such that $d_1 \leq \frac{1}{\|x\|} \leq d_2$, then by (3.14) we get $d_1 |\nabla_a E\mu(a)| \leq |\nabla_x E\mu(x)| \leq d_2 |\nabla_a E\mu(a)|$. Thus,

$$\begin{aligned} \int_{\mathcal{K}} |\nabla_{\mathcal{S}} \mu|^2 &= \int_{\mathcal{K}} |\nabla E\mu|^2 \\ &= \int_{\mathcal{K}_h} |\nabla E\mu \circ \mathcal{P})|^2 |J| \\ &\leq \frac{c_1}{d_1} \int_{\mathcal{K}_h} |\nabla v|^2. \end{aligned}$$

So, there exists some constants $c_3 > 0$, and $c_4 > 0$ such that

$$c_3 \|v\|_{H^1(\mathcal{K}_h)} \leq \|\mu\|_{H^1(\mathcal{K})} \leq c_4 \|v\|_{H^1(\mathcal{K}_h)}.$$

Taking the gradient of both sides of (3.14), we get

$$\nabla_x^2 E\mu(x) = \nabla_x \left(\frac{1}{\|x\|} \right) \nabla_a E\mu(a) + \frac{1}{\|x\|^2} \mathbf{A} \nabla_a \left(\nabla_a E\mu(a) \right).$$

So for some constant c_5 we get the following estimate,

$$|v|_{H^2(\mathcal{K}_h)} \leq c_5 \|\mu\|_{H^2(\mathcal{K})}.$$

□

Let $\mathcal{I}$ denote the linear interpolation operator for continuous functions defined on $\mathcal{S}$, then $\mathcal{I}\mu(a) = \sum_{i=1}^{m} \mu(\eta_i)\varphi_i(a)$ is uniquely determined by the interpolation conditions. Denote the restriction of $\mathcal{I}$ to the spherical triangle $\mathcal{K}$ by $\mathcal{I}_T = \mathcal{I}|_{\mathcal{T}}$, then $I_T\mu = \sum_{i=1}^{3} \mu(\eta_i)\varphi_i$. Let I_h denote the linear interpolation operator for continuous functions defined on Ω, then $I_h u(x) = \sum_{i=1}^{m} u(\eta_i)\phi_i(x)$, is also uniquely determined by the interpolation conditions. Similarly, let $\mathcal{I}_{\mathcal{K}_h} = \mathcal{I}_h|_{\mathcal{K}_h}$ denote the restriction of $\mathcal{I}_h$ onto the planar triangle $\mathcal{K}_h$. The linear interpolation operator $\mathcal{I}_h$ on Ω and interpolation operator $\mathcal{I}$ on $\mathcal{S}$ are related to each other, in particular

$$\mathcal{I} = \mathcal{I}_h \circ \mathcal{P}^{-1}.$$

Theorem 3.2 *Let $\mu \in H^2(\mathcal{S})$, then we have the following estimates*

$$\|\mu - \mu_h\|_{L^2(\mathcal{K})} \leq h^2 \|\mu\|_{H^2(\mathcal{K})},$$

and

$$\|\mu - \mu_h\|_{H^1(\mathcal{K})} \leq h \|\mu\|_{H^2(\mathcal{K})}$$

Proof:

$$\begin{aligned}
\|\mu - \mu_h\|_{H^1(\mathcal{K})} &\leq \|\mu - \mathcal{I}_{\mathcal{K}}\mu\|_{H^1(\mathcal{K})}, \\
&\leq c\|u - \mathcal{I}_{\mathcal{K}_h}u\|_{H^1(\mathcal{K}_h)}, \\
&\leq ch|u|_{H^2(\mathcal{K}_h)}, \\
&\leq ch\|\mu\|_{H^2(\mathcal{K})}.
\end{aligned}$$

Similarly,

$$\begin{aligned}
\|\mu - \mu_h\|_{L^2(\mathcal{K})} &\leq ch\|\mu - \mu_h\|_{H^1(\mathcal{K})}, \\
&\leq ch^2\|\mu\|_{H^2(\mathcal{K})}.
\end{aligned}$$

□

Chapter 4

Numerical Experimetns

4.1 Finite elements on the sphere

Consider the unit sphere, $\mathcal{S}$ of $\mathbb{R}^3$, centered at the origin and consider the box $\mathcal{B}$ in $\mathbb{R}^3$, with side length 2 which is also centered at the origin. Let $\{\mathcal{K}_1, \ldots, \mathcal{K}_n\}$ denote a triangulation of the box and recall that the box is radially projected onto the sphere. Let $\{\mathcal{T}_1, \ldots, \mathcal{T}_n\}$ denote the corresponding finite element discretization of the sphere.

For simplicity, we use linear finite elements for the box, so χ_h denotes the finite element space of the box such that it consists of piecewise linear continuous polynomials: $\chi_h = \{v : \mathcal{B} \to \mathbb{R}$ s.t. v is a piece wise continuous linear polynomial $\}$. Let $\{\xi_i\}_{i=1}^m$ denote nodes of the finite element discretization of the box and let $\{\phi_i\}_{i=1}^m$ denote the basis functions of the finite element space χ_h with $\phi_i(\xi_j) = \delta_{ij}$ where δ_{ij} is the Kronecker-delta. The support of the basis function ϕ_i consists of all the triangles which share the node ξ_i. Since, ϕ_i are linear basis functions, for any point $x = (x_1, x_2, x_3)$ on the box, we have $\phi_i(x_1, x_2, x_3) = kx_1 + mx_2 + nx_3 + d$ for some constants k,m,n and d. For example, if $x = (x_1, x_2, x_3)$ is on $\mathcal{F}_1$, then $\phi_i(1, x_2, x_3) = mx_2 + nx_3 + c$

Let χ denote the finite element space on the unit sphere. We denote the basis function of χ by $\{\varphi_i\}_{i=1}^m$. Let a be any point on the sphere then there exists a point x on the box with $\mathcal{P}(x) = a$, we define the basis functions on the sphere as $\varphi_i = \phi_i \circ \mathcal{P}^{-1}$. For example, let the inverse projection of $a = (a_1, a_2, a_3)$ be on the face $\mathcal{F}_1$, then $\varphi_i(a_1, a_2, a_3) = \phi_i(1, \frac{a_2}{a_1}, \frac{a_3}{a_1}) = m\frac{a_2}{a_1} + n\frac{a_3}{a_1} + c$. So, the basis functions on the sphere are rational functions. Figure (4.1) shows a basis function on the sphere.

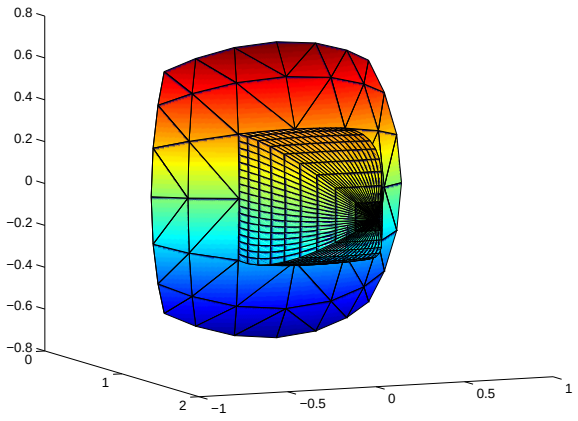

Figure 4.1: Basis functions on the sphere

4.2 Example 1

To illustrate our method and to verify the theoretical results, we present numerical experiments for the following model problem

$$-\Delta_{\mathcal{S}}\mu + \mu = f, \text{ on } \mathcal{S}.$$

We choose a classical solution of the above problem to be $\mu(a_1, a_2, a_3) = \cos a_1$, then we calculate the right hand side, f by

$$f = -\nabla_{\mathcal{S}} \cdot \nabla_{\mathcal{S}} + \mu, \quad \nabla_{\mathcal{S}} = \nabla\mu - (\nabla\mu \cdot n)n \quad -\nabla_{\mathcal{S}} \cdot \nabla_{\mathcal{S}} = \nabla \cdot \nabla_{\mathcal{S}} - \sum_{i=1}^{3} (\nabla_{\mathcal{S},i} \cdot n)n_i \quad (4.1)$$

and get that $f(a) = a_1^4 cos(a_1) - (1 + a_1^2)a_1^2 cos(a_1) + 2cos(a_1) + 2a_1^3 sin(a_1) - (2 + 2a - 1^2)a_1 sin(a_1)$. We denote by μ_h the approximate solution, and by h the largest diameter of

the spherical triangles at the j^{th} refinement step. The experimentally observed convergence rate, p is

$$p = \frac{\ln\left(\frac{E^j}{E^{j+1}}\right)}{\ln\left(\frac{h^j}{h^{j+1}}\right)},$$

where E^j denotes the error in the L^2-norm at j^{th} refinement step. Similarly, q is the experimentally observed convergence rate when the error is measured in the H^1-norm. We present the results in the following table (4.2).

j	n	h	$\|\mu - \mu_h\|_{L^2(\mathcal{S})}$	p	$\|\mu - \mu_h\|_{H^1(\mathcal{S})}$	q
1	48	0.9553	0.0439	-	0.3466	-
2	192	0.6155	0.0300	0.8661	0.2763	0.5157
3	768	0.3398	0.0087	2.0837	0.1478	1.0531
4	3072	0.1750	0.0023	2.0049	0.0757	1.0083
5	12288	0.0882	0.0005848	1.9986	0.0382	0.9982
6	49152	0.0441	0.000147	1.9987	0.0191	1.0033
7	196,608	0.0221	0.000036799	1.9981	0.0096	0.9925

Table 4.1: Numerical results.

In this table j denotes the refinement step, h denotes the largest diameter of the spherical triangles measured using geodesic distance formula (2.5), n deontes the number of spherical triangles, p denotes the experimentally observed convergence rate in the L^2-norm, and q denotes the experimentally observed convergence rate in the H^1-norm . Figure (4.2) is a plot of the approximate solution μ_h.

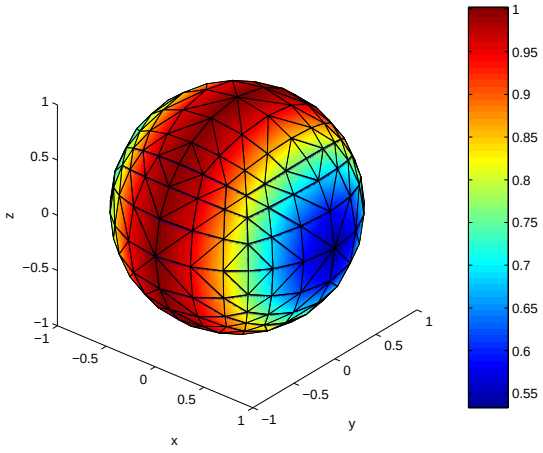

Figure 4.2: Numerical approximation to $\mu(a) = cosa_1$.

4.3 Example 2

Next consider the following second order elliptic equation defined on the ellipsoid, whose equation is given by $a_1^2 + \frac{a_2^2}{4} + \frac{a_3^2}{4} = 1$

$$-\Delta_{\mathcal{E}}\mu + \mu = f, \text{ on } \mathcal{E}.$$

We chose the exact solution to be $\mu(a) = cos(a_1)$, then the right hand side f is calculated by using (4.1), where $n = (2a_1^2, \frac{2a_2^2}{4}, \frac{2a_3^2}{4})$. As in the previous example, μ_h denotes the approximate solution, and h denotes the largest diameter of the finite element at the j^{th} refinement step. We calculate the experimentally observed convergence rate and the results are presented in table (4.3).

j	n	h	$\|\mu - \mu_h\|_{L^2(\mathcal{S})}$	p	$\|\mu - \mu_h\|_{H^1(\mathcal{S})}$	q
1	48	0.9553	0.0439	-	0.3466	-
2	192	0.6155	0.0300	0.8661	0.2763	0.5157
3	768	0.3398	0.0087	2.0837	0.1478	1.0531
4	3072	0.1750	0.0023	2.0049	0.0757	1.0083
5	12288	0.0882	0.0005848	1.9986	0.0382	0.9982
6	49152	0.0441	0.000147	1.9987	0.0191	1.0033
7	196,608	0.0221	0.000036799	1.9981	0.0096	0.9925

Table 4.2: Numerical results

4.4 Example 3

Consider the following eigenvalue problem,

$$-\Delta_{\mathrm{S}}\mu = \lambda\mu. \tag{4.2}$$

Eigenvalues of the problem (4.2) are $\lambda_k = k(k+1)$ $k = 0, 1, \ldots$ and the eigenvalue λ_k has a multiplicity of $2k+1$. Galerkin approximation of the variational problem is find $\lambda^h \in \mathbb{R}$ and $0 \neq \mu^h \in \chi$ s.t.

$$a_h(\mu^h, \nu^h) = \lambda^h(\mu^h, \nu^h)\ \forall \nu^h \in \chi.$$

Here $a_h(\cdot,\cdot)$ is as in (1.15) and χ is as in (3.5). Exact eigenvalues $2, 6, 12, 20$ and their approximates with the finite element method is presented in table (4.4). Here n denotes the number of elements in each refinement step.

n	2	6	12	20
	2.2325	6.5237	14.8632	29.3408
	2.2325	6.5237	18.3974	30.1297
	2.2325	9.015	18.3974	30.1297
		9.015	18.3974	35.6114
48		9.015	22.2659	35.6114
			22.2659	35.6114
			22.2659	35.6114
				51.311
				51.311
				51.311
	2.0568	6.3224	13.437	24.192
	2.0568	6.3224	13.656	24.192
	2.0568	6.5956	13.656	24.385
		6.5956	13.656	25.108
192		6.5956	14.362	25.108
			14.362	25.108
			14.362	26.483
				26.483
				26.483
	2.0146	6.0912	12.416	21.248
	2.0146	6.0912	12.444	21.248
	2.0146	6.1491	12.444	21.341
		6.1491	12.444	21.341
768		6.1491	12.581	21.341
			12.581	21.371
			12.581	21.502
				21.502
				21.502
	2.0037	6.0239	12.107	20.324
	2.0037	6.0239	12.115	20.324
	2.0037	6.0375	12.115	20.341
		6.0375	12.115	20.341
3072		6.0375	12.146	20.341
			12.146	20.358
			12.146	20.376
				20.376
				20.376

Table 4.3: Exact eigenvalues and their approximates

2		6		12		20	
e_{min}/e_{max}	p_{min}/p_{max}	e_{min}/e_{max}	$p_{min}/\ p_{max}$	e_{min}/e_{max}	p_{min}/p_{max}	e_{min}/e_{max}	p_{min}/p_{max}
0.2325/ 0.2325		0.5237 / 3.015		2.8632/10.266		9.3408/31.311	
0.0568/0.0568	3.2061/3.2061	0.3224/0.5956	1.1036/3.6893	1.437/2.362	1.5682/3.3425	4.192 /6.483	1.8226/3.5824
0.0146/ 0.0146	2.2868/2.2868	0.0912/0.1491	2.1255 / 2.3313	0.416 /0.581	2.0866/ 2.3608	1.248/1.502	2.0395/2.4616
0.0037/ 0.0037	2.0686/2.0686	0.0239/0.0375	2.0181/2.0801	0.107/0.146	2.0463/2.0814	0.324/0.376	2.0323/2.0871

Table 4.4: Experimentally calculated convergence rates.

Chapter 5

Conclusion

We developed and analyzed a new method for exactly discretizing spheroidal domains and constructing finite element spaces on such domains, thus yielding conforming finite element discretizations. This method may be used to approximate solutions of partial differential equations, as well as eigenvalues and eigenfunctions of differential operators defined on such domains (spherical, ellipsoidal, cylindrical, and toroidal shells). This method which was described for the Laplace-Beltrami equation can be easily generalized to approximate solutions of other partial differential equations and eigenvalue problems defined on the spheroidal domains. The methods is easy to implement and can be easily incorporated into existing finite element codes. Moreover, the method can be generalized to other convex domains by means of generalized projections, provided these are available analytically.

Bibliography

[1] Denis Barden and Charles Thomas, "An Introduction to Differential Manifolds", Imperial College Press, 2005.

[2] John M. Lee, "Introduction to Smooth Manifolds", Springer, 2002.

[3] J. Wloka, "Partial differential equations", Cambridge University Press, 1987.

[4] P.E. Ciarlet, "The Finite Element Method for Elliptic Problems," SIAM, 2002.

[5] Gilbert Strang, George Fix, "An Analysis of the Finite Element Method ," Prentice-Hall, 1973.

[6] Ronchi, C.; Paolucci, P. S., The "cubed sphere": a new method for the solution of partial differential equations in spherical geometry, *J. Comput. Phys.*, **124**(1996), 93-114.

[7] Qiang Du, Lili Ju, "Finite volume methods on spheres and spherical centroidal voronoi meshes", *SIAM Journal on Numerical Analysis,* **43**, (2005),1673-1692.

[8] D. Gilbarg, N.S. Trudinger " Elliptic partial differential equations of second order",Springer, 1977.

[9] Gerhard Dziuk, Finite elements for the Beltrami operator on arbitrary surfaces.*Partial differential equations and calculus of variations*, 142-155, Lecture Notes in Math., 1357, Springer, Berlin, 1988.

[10] John R. Baumgardner; Paul O. Frederickson, Icosahedral Discretization of the Two-Sphere, *SIAM Journal on Numerical Analysis,* **22** (1985) 1107-1115.

[11] Dietrich Braess, "Finite elements. Theory, fast solvers, and applications in solid mechanics", Cambridge, 2001.

[12] Susanne Brenner, L. Ridgway Scott " The mathematical theory of finite element methods", Springer, Verlag, 1994.

[13] Andrew V. Knyazev, John E. Osborn New a priori FEM error estimates for eigenvalues, *SIAM Journal on Numerical Analysis,* **43**(2006),2647-2667.

[14] I. Babuska, J.E. Osborn Estimated for the errors in eigenvalue and eigenvector approximation by Galerikin methods, with particular attention to the case of multiple eigenvalues. *SIAM Journal on Numerical Analysis,* **24**(1987)1249-1276.

[15] I. Babuska, J.E. Osborn Finite element-Galerkin approximation of the eigenvalues and eigenvectors of selfadjoint problems. *Mathematics of Computation,***52**(1989)275-297.

[16] Thierry Aubin *Nonlinear Analysis on manifolds. Monge-Ampère Equations*, Springer-Verlag, 1982.